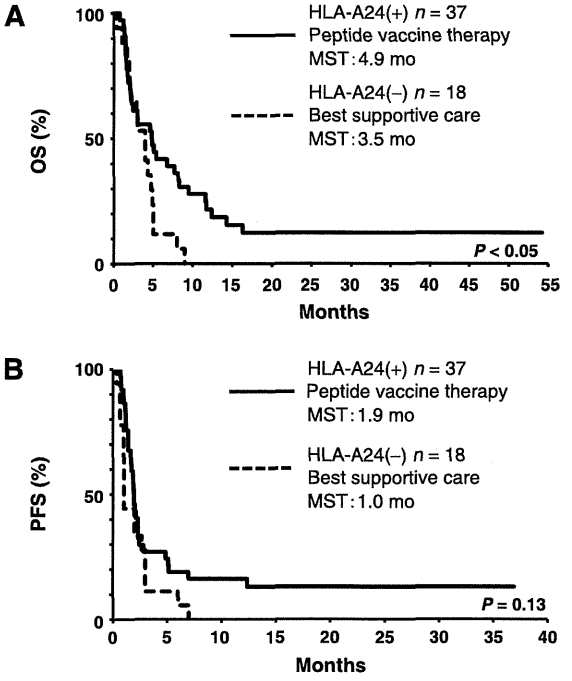

Figure 1.
OS and PFS of the HLA-A24(+) and HLA-A24(−) groups. The HLA-A24(+) patients received peptide vaccination, whereas the HLA-A24(−) patients did not. The OS (A) and PFS (B) were evaluated in the HLA-A24 (*HLA-A*24:02*)-positive patients treated with peptide vaccination and the HLA-A24-negative patients treated without peptide vaccination for the subgroup analysis. The OS and PFS were analyzed according to the Kaplan–Meier method, and statistical differences were assessed using the log-rank test.

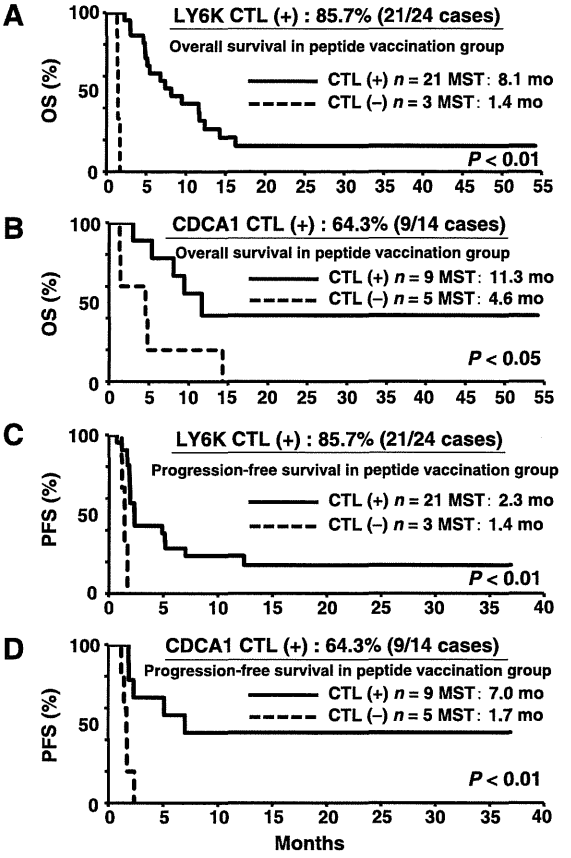

Figure 2.
A prolonged OS and PFS in the HLA-A24(+) group were correlated with a CTL response specific to each of the LY6K and CDCA1 peptides. In the HLA-A24 (+) group, *in vitro* cultured T cells were subjected to ELISPOT assays. Positive CTL responses specific to LY6K- and CDCA1 peptides after vaccination were observed in 85.7% and 64.3% of the patients, respectively. The OS was compared between the patients with a positive CTL response [CTL (+)] and those with a negative CTL response [CTL (−)] to each peptide, and the patients with a positive CTL response specific to the LY6K peptide were found to exhibit a significantly longer OS and PFS than those without a CTL response (A and C). Similarly, the patients with a positive CTL response specific to the CDCA1 peptide showed a significantly longer OS and PFS than those without a CTL response (B and D).

the 37 patients, 1 (case 18) was judged to have achieved a complete response (CR) for 37 months and nine were found to have stable disease (SD) for 3 months, according to the RECIST criteria. The disease control rate (CR+SD) was 27.0% after 3 months. The median time to PFS was 1.9 months. The median OS was 4.9 months.

When the patients were classified into A24(+) and A24 (−) groups, the OS of the A24(+) group was statistically significantly longer than that of the A24(−) group (4.9 vs. 3.5 months at MST, respectively; $P < 0.05$; Fig. 1A). The PFS of the A24(+) group was not significantly better than that of the A24(−) group (1.9 vs. 1.0 months at MST, respectively; $P = 0.13$; Fig. 1B).

Prolonged OS in the A24(+) group correlated with specific CTL responses

In the A24(+) group, *in vitro* cultured T cells were subjected to ELISPOT and pentamer assays, and positive CTL responses specific for the LY6K-, CDCA1-, and IMP3 peptides after vaccination were observed in 85.7%, 64.3%, and 42.9% of the patients, respectively. When the OS was compared between the A24(+) patients in the CTL response-positive and -negative groups, the patients showing a CTL response specific to the LY6K peptide exhibited a significantly longer OS than those without an LY6K-specific CTL response (Fig. 2A). Similarly, the patients demonstrating a positive response specific to the CDCA1 peptide exhibited a significantly longer OS than those without a CTL response (Fig. 2B). The OS of the patients with an IMP3-specific CTL response tended to be longer than that of the patients without a CTL response, although the difference was not statistically significant. The PFS of the patients with LY6K-, CDCA1-, and IMP3-specific CTL responses tended to be longer than that of the patients without CTL responses (Fig. 2C and D). Interestingly, when the patients were divided into four groups according to the number of antigenic peptides to which they showed a positive CTL response, the OS was longer in the groups in which the patients demonstrated a positive CTL response to a larger number of peptides (Fig. 3); the MST of the patients exhibiting CTL responses to three peptides was longer (19.5 months) than that observed in the other patient groups (Fig. 3). These observations indicate that the immunologic response induced by the peptide vaccination contributed to improving the prognosis of these patients.

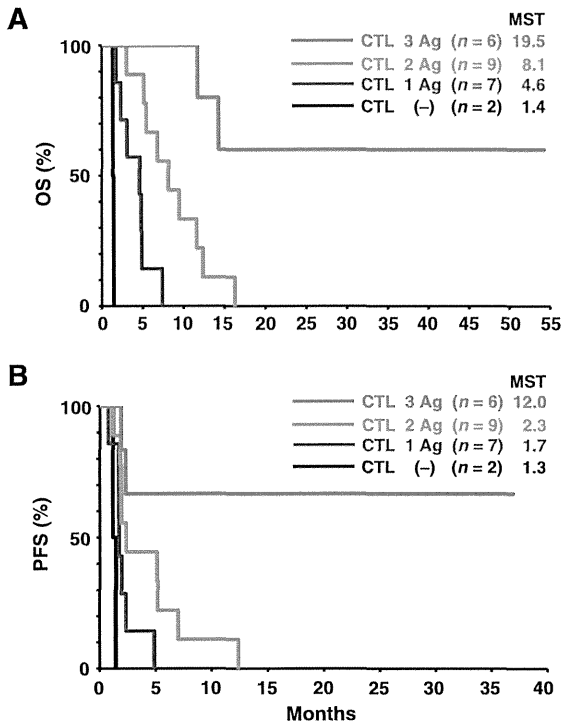

Figure 3.
OS of the four subgroups of HLA-A24(+) patients receiving peptide vaccination classified according to the number of peptides inducing a positive CTL response. The HLA-A24(+) patients were classified into four groups according to the number of peptide antigens (0, 1, 2, or 3) inducing a CTL response. A, the OS tended to increase as the number of peptides inducing a CTL response increased. B, the PFS exhibited a similar tendency to the OS.

The results of the representative ELISPOT and pentamer assays specific to the LY6K peptide are shown in Fig. 4. The ELISPOT assay indicated substantial T-cell responses specific to the LY6K peptide in comparison with the irrelevant peptide (Supplementary Fig. S1A), according to the criteria described in Materials and Methods. This LY6K-specific T-cell response was further confirmed by the LY6K-pentamer assay, as shown in Supplementary Fig. S1C, with a proportion of 27.0% of pentamer$^+$ CD8$^+$ cells among CD3$^+$ T cells. Moreover, the infiltration of CD8$^+$ T cells into the tumor tissue increased after vaccination (Supplementary Fig. S1D). Tumor biopsies were performed with informed written consent before vaccination and at the time of recurrence after vaccination.

The detailed chronological changes of CTL responses checked at before vaccination, the fourth and the eighth vaccinations among 24 cases investigated are shown in Supplementary Fig. S2A. In 20 cases out of 22 cases, CTL responses increased depending on increased vaccinations, whereas CTL response decreased in 2 cases. In 1 of those cases, CTL response decreased after the eighth vaccination, but the strong CTL response was observed after the 12th and the 16th vaccinations (data not shown). This observation may be due to the timing of blood sampling when the patients' physical condition became worse after the eighth vaccination. We thought that CTL response is accidentally undetectable only at the eighth vaccination, thereafter induction of CTL in this patient has been observed after repeated vaccinations. In terms of the correlation between positive pentamer responses and positive ELISPOT responses, positive correlation was observed in 2 cases. We showed the results of the case 24 in Supplementary Fig. S2B.

There is only 1 case from whom tumor tissue specimens can be collected after vaccination. We confirmed the expression of HLA class I before and after the vaccination. As a result, the expression level was not changed much, expression loss of TAAs has not been observed.

Adverse reactions

The peptide vaccine therapy was well tolerated without any treatment-associated adverse events of grade 3 or higher. Twenty-eight of the 37 patients developed grade 1 or 2 local skin reactions with redness, induration, swelling, and pruritus at the injection site. No high-grade fevers, fatigue, diarrhea, headaches, rashes, or itching were observed in any of the patients, and no hematologic, cardiovascular, hepatic, or renal toxicity was observed during or after vaccination. The adverse events observed in this trial are listed in Table 2.

Skin reactions, OS, and PFS

Skin reactions were observed after vaccination in 75.7% of all enrolled patients. The OS and PFS of the skin reaction–positive and -negative patients are shown in Fig. 5A and B. The OS of the skin reaction–positive group was statistically significantly longer than that of the skin reaction–negative group (7.1 vs. 1.4 months at MST, respectively; $P < 0.01$; Fig. 5A). Moreover, the PFS of the skin reaction–positive group was statistically significantly longer than that of the skin reaction–negative group (2.3 vs. 1.2 months at MST, respectively; $P < 0.01$; Fig. 5B).

A case of CR following peptide vaccination

The patient in case 18 developed tongue cancer recurrence and lymph node metastasis on the right side of her neck 15 months after surgery. Initially, she received S-1 chemoradiotherapy at a daily dose of 80 mg for 14 days and irradiation (a total of 40 Gy) for 20 days in addition to two cycles of chemotherapy with docetaxel (80 mg) and cisplatin (90 mg) as adjuvant therapy. Despite receiving these treatments, the patient's tumors did not disappear. Therefore, we decided to administer our peptide vaccine therapy. The amount of purulent discharge and swelling on the right side of the neck decreased to a normal state after 12 vaccinations, and the symptoms of tumor recurrence and neck lymph node metastasis disappeared after 16 vaccinations (Fig. 4C). The frequency of pentamer-positive CTL increased after vaccination (from 0.01% to 6.0%), and an ELISPOT assay showed that the LY6K peptide-specific CTL response increased after 16 vaccinations (Fig. 4A and B). At present, 37 months after the initiation of peptide vaccination, the patient has been remained free of tumor recurrence and metastasis.

Discussion

In the present phase II clinical study, we demonstrated that the CT antigenic peptide-based vaccination-induced immune response is positively correlated with a better prognosis in patients with advanced and inoperable HNSCC. In addition, cancer vaccination using a combination of multi-epitope peptides as monotherapy may provide a clinical benefit for patients. To our knowledge, this study is the first to show a promising result indicating that

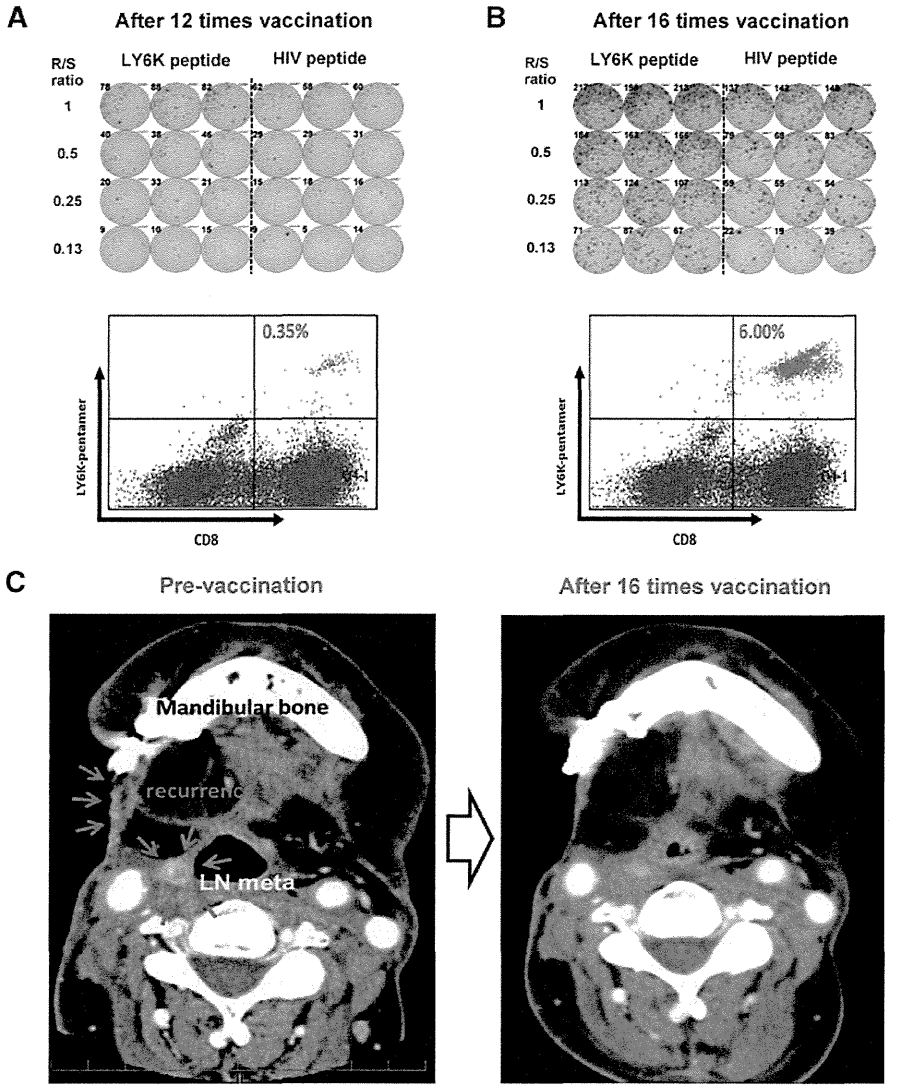

Figure 4.
CT imaging of the recurrent and metastatic tumors in case 18, in which the clinical response to vaccination was judged to be a CR. A and B, PBMCs obtained from the patient in case 18 (*HLA-A*24:02*-positive) after the 12th and 16th vaccinations were cultured in rIL2 for 14 days with two episodes of LY6K peptide stimulation. The cultured lymphocytes were subjected to an ELISPOT assay following the depletion of CD4-positive cells using magnetic beads. The results of immunologic monitoring assays using an ELISPOT assay and flow cytometry with the HLA-A24/LY6K-pentamer in combination with anti-CD8 and anti-CD3 mAbs are presented at the time points after 12 (A) and 16 (B) vaccinations in case 18. The LY6K-specific CTL response increased after 16 vaccinations. C, CT imaging showed tumor recurrence and lymph node metastasis before vaccination. After 16 cycles of vaccination, the recurrent and metastatic tumors disappeared, and the patient was judged to have exhibited a CR on CT imaging by a radiologist. It has been 3 years since the tumor and metastatic lymph node lesions disappeared.

therapeutic cancer vaccination with multiple peptides can potentially improve the prognosis of patients with advanced HNSCC refractory to standard therapy.

Several phase II and III clinical trials have recently demonstrated promising and therapeutic results of cancer vaccination (19, 24–32). However, most of these studies were performed using single antigen-based vaccination with several modifications, and the clinical benefits appeared to be limited. To further improve the clinical response to cancer vaccination, it is necessary to consider the application of a combination of multiple peptide vaccines derived from different TAAs, as such therapy may overcome problems associated with the heterogeneity of tumor cells and escape of tumor cells from the peptide-specific immune response due to the loss of an antigen expression (28, 33). In general, the preferable characteristics of target molecules for the development of cancer vaccines include (i) a high level of immunogenicity, (ii) a common and high expression in cancer cells, (iii) a specific expression in cancer cells, testis or fetal tissues only, and (iv) the presence of essential molecules for cell division and survival (to prevent a loss of expression; refs. 28, 33). In this regard, the LY6K, CDCA1, and IMP3 molecules used in the present trials are considered to be the most appropriate because they have already been proven to be cancer–testis antigens satisfying all four ideal characteristics described above (13–16, 34–36) and are expressed in the majority of HNSCC cells. This study was the first report of peptide vaccine therapy for patients with HNSCC. We administrated mixed peptide vaccine, so CTL was more inducible as compared with using only one peptide. OS was significantly prolonged, the patient who responded to the three peptides than one peptide. In the future, we want to develop the peptide vaccine therapy that can reject the cancer cells more strongly.

In the present phase II clinical trial, we compared the OS and PFS between a A24(+) group treated with peptide vaccination and an A24(−) group treated without peptide vaccination. The OS

Table 2. The incidence of adverse events

	Total (%)
Any events	28 (75.7)
Any immune-related events	28 (75.7)
Drug fever	3 (8.1)
Rash or flushing	0 (0)
Injection site reaction (redness, induration, ulceration)	25 (67.6)
Pruritus	27 (73.0)
Blood disorders	0 (0)
Leukopenia	0 (0)
Neutropenia	0 (0)
Anemia	0 (0)
Thrombopenia	0 (0)
Increase in PT-INR[a]	0 (0)
Hepatic disorders	0 (0)
Hyperbilirubinemia	0 (0)
Increase in serum aspartate aminotransferase	0 (0)
Increase in serum alanine aminotransferase	0 (0)
Renal disorders	0 (0)
Increase in serum creatinine	0 (0)
Proteinuria	0 (0)

[a]PT-INR, prothrombin time-international normalized ratio.

and, less significantly, PFS in the A24(+) group treated with peptide vaccination were longer than those observed in the A24(−) group treated without peptide vaccination, suggesting that therapeutic cancer vaccine treatment using peptides inducing

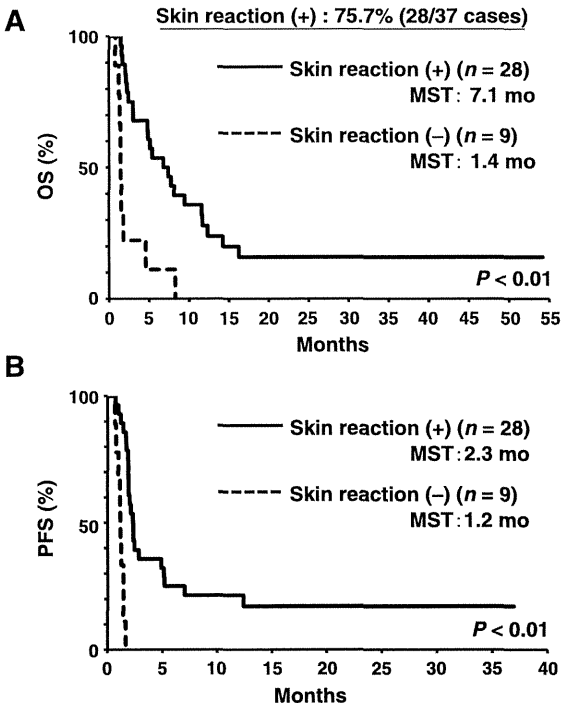

Figure 5.
The occurrence of skin reactions was correlated with the prolongation of OS and PFS. The patients with skin reactions (+) exhibited longer OS (A) and PFS (B) with statistical significance than those without skin reactions (−). The MST of the OS of the patients with skin reactions (+) versus those without (−) was 7.1 vs. 1.4 months, respectively. The MST of the PFS of the patients with skin reactions (+) vs. those without (−) was 2.3 vs. 1.2 months, respectively.

HLA-A24–restricted CTLs may provide a survival benefit in patients with advanced HNSCC. Furthermore, as demonstrated in the A24(+) group, specific CTL responses to two or three peptides may improve the OS in comparison with that observed in patients with CTL induction to no or only a single peptide. Although treatment with cancer vaccination has been shown to result in increased levels of circulating tumor antigen-specific T cells (37), we herein provided direct evidence of a positive correlation between the extent of the peptide-specific CTL response and a longer OS. Therefore, the findings of the present study support the hypothesis that peptide vaccination-induced immune responses contribute to improving the prognosis of patients with advanced HNSCC.

According to the recommendation by the iSBSTc-SITC/FDA/NCI Workshop on Immunotherapy Biomarkers (38–40), we carried out immunologic monitoring in the A24(+) group treated with peptide vaccination using two different assays, ELISPOT and pentamer assays, at three different time points at a central laboratory. Because the peptides used in the present study exhibited strong immunogenicity, *in vitro* immunologic monitoring in the A24(+) group was successfully performed in a reliable fashion.

In this clinical trial, we used a vaccine containing 3 mg of peptides in total, among which 1 mg of each of three peptides was mixed, in an attempt to activate CTL responses against tumor cells. Previously, Nakatsura and colleagues reported the use of Glypican-3–derived peptide vaccination (Glypican-3 is an oncofetal antigen that is overexpressed in hepatocellular carcinoma cells). The authors were able to induce a Glypican-3–specific CTL response dose-dependently (41). In addition, considering the amount and effect of intradermal administration, good results were obtained with 3 or 10 mg of peptides. Therefore, in performing our peptide vaccination trial using mixed peptides derived from tumor-specific antigens, we prepared 3 mg of peptides in total. As a result, the patients exhibiting a CTL response against three and two peptides demonstrated an extended OS in comparison with those exhibiting a CTL response against none or only one peptide. This finding suggests that the effects of peptide vaccination are observed in patients with some precursor T cells against TAAs. In 13 of the 15 patients who were not evaluated for a CTL response, we were unable to obtain blood samples for the CTL analysis because they received less than four peptide vaccinations. In addition, it was observed that 15 of the 37 patients exhibited CTL induction against two or three types of peptides, suggesting that the individual peptides used for vaccination do not inhibit the CTL induction of each other. There is a possibility that some patients will exhibit induced CTL responses to all peptides used for vaccination if the number of patients tested is further increased. On the other hand, in the peripheral blood collected from patients vaccinated with these peptides, increased responses of $CD4^+$ T cells reactive to the same and other TAA-derived peptides have been observed (42, 43). These phenomena may be explained by the activation of $CD4^+$ T cells exposed to TAAs released from tumor cells killed by CTLs in the presence of dendritic cells that can uptake and process TAAs into antigenic peptides recognized by $CD4^+$ T cells.

We analyzed the frequencies of Treg cells before and after vaccinations in 5 patients (Supplementary Fig. S3). In 2 patients (cases 1 and 3), the high proportions of Treg cells were observed pre- and postvaccination, and CTL was induced by only one

peptide. On the other hand, in 2 patients (cases 2 and 4), the low proportions of Treg cells were observed pre- and postvaccination, and CTLs were induced by all the three peptides. Furthermore, in 1 patient (case 5) who showed increased proportion of Treg cells postvaccination, peptides-specific CTLs were not induced by the vaccination. Considering from these results, it is suggested that it may be difficult to induce CTL in patients with high proportion of Treg cells before vaccination. On the other hand, in patients with low proportion of Treg cells before vaccination, it may be possible to induce CTL. Because the peptide-specific CTLs were not induced in 1 patient who showed significant increase of Treg cells after vaccination even though Treg cell proportion was not so high before vaccination, there may be a possibility that CTL could not be well induced in the presence of increased Treg cells. In any case, we have to investigate Treg cell status in more patients to make a conclusion of this question in future.

In the present study, 1 patient (case 18) achieved a clinical CR. This finding demonstrates that our peptide vaccination can yield an excellent response in some patients with HNC. The patient had received adjuvant chemotherapy with limited systemic chemotherapy for 3 months before vaccination. She was evaluated to have a PS of 1 according to the ECOG classification, with a WBC count of 6,000/μL and a lymphocyte level of 1,300/μL. In this case, the number of LY6K-specific $CD8^+$ T cells finally increased at 5 months after the start of peptide vaccination, and the LY6K-peptide specific CTL response increased to 6% by *in vitro* stimulation approximately 8 months later. At the same time, disappearance of the patient's tumor recurrence and neck lymph node metastasis was confirmed on a CT examination. Since then, no tumor recurrence has been observed for 3 years. An ELISPOT assay was used to detect a CTL response against the LY6K peptide 2 years after the start of vaccination, and we considered the patient to have obtained the successful induction of memory T cells against the peptides.

Recently, there was a report that persisting peptide/IFA vaccine depots can induce specific T-cell sequestration, dysfunction, and deletion at the site of vaccination in mice (44). In this clinical study, we experienced a patient who was vaccinated 61 times during an approximately 4-year period, with good induction of peptide-specific CTL responses. The patient was in a tumor-bearing state and received a significant dose of peptide vaccination. This may be why the patient demonstrated a peptide-specific CTL response for such a long period. In addition, the degree of T-cell sequestration and dysfunction may differ depending on the type of tumor-associated antigen or based on differences between humans and mice.

Because available cancer vaccines are likely to be applied as adjuvant treatment in patients at a high risk of recurrence following surgical resection of the primary tumor (28, 33), we are planning to develop a cancer peptide vaccine for use in the treatment of patients with HNC in the adjuvant setting. However, even if the patient is at an advanced stage of the disease and has received intensive treatment with chemotherapy and/or radiotherapy, the present study indicates that cancer peptide vaccination may provide some clinical benefit as monotherapy without severe adverse effects. In general, there is no curative therapy for HNSCC associated with inoperable tumors or recurrence after surgery. Hence, we believe that our protocol is promising for improving the prognosis and quality of life, at least for some fraction of patients with advanced HNSCC.

Conclusion

To our knowledge, this study is the first to show the proof of concept that CT antigenic peptide-based vaccination-induced immune responses are associated with better prognoses in patients with advanced HNSCC, implying that cancer vaccination with multiple peptides as monotherapy may provide hope for patients with advanced and/or inoperable HNSCC refractory to standard therapy.

Disclosure of Potential Conflicts of Interest

K. Yoshida is an employee of OncoTherapy Science, Inc. Y. Nishimura reports receiving a commercial research grant from OncoTherapy Science, Inc. Y. Nakamura reports receiving a commercial research grant from and has ownership interest (including patents) in OncoTherapy Science, Inc. No potential conflicts of interest were disclosed by the other authors.

Authors' Contributions

Conception and design: Y. Yoshitake, Y. Nakamura
Development of methodology: Y. Yoshitake, H. Jono, K. Yoshida
Acquisition of data (provided animals, acquired and managed patients, provided facilities, etc.): Y. Yoshitake, D. Fukuma, A. Yuno, M. Hirayama, H. Nakayama, T. Tanaka, M. Nagata, Y. Takamune, K. Kawahara, Y. Nakagawa, R. Yoshida, A. Hirosue, H. Ogi, A. Hiraki, A. Hamada
Analysis and interpretation of data (e.g., statistical analysis, biostatistics, computational analysis): Y. Yoshitake, A. Hamada
Writing, review, and/or revision of the manuscript: Y. Yoshitake, A. Yuno, Y. Nishimura
Administrative, technical, or material support (i.e., reporting or organizing data, constructing databases): Y. Yoshitake, H. Jono, Y. Nishimura
Study supervision: Y. Nishimura, Y. Nakamura, M. Shinohara

Acknowledgments

The authors thank Dr. Takuya Tsunoda, Laboratory of Molecular Medicine, Human Genome Center, Institute of Medical Science, and University of Tokyo for their excellent advice and cooperation and for providing all of the peptides.

Grant Support

This research was supported by JSPS KAKENHI Grant Number 23792363 to Y. Yoshitake, an MEXT KAKENHI Grant Number 22133005, JSPS KAKENHI Grant Number 24300334 to Y. Nishimura, and funding to Y. Nishimura from OncoTherapy Science, Inc.

The costs of publication of this article were defrayed in part by the payment of page charges. This article must therefore be hereby marked *advertisement* in accordance with 18 U.S.C. Section 1734 solely to indicate this fact.

Received January 24, 2014; revised September 23, 2014; accepted October 18, 2014; published OnlineFirst November 12, 2014.

References

1. Ferlay J, Shin HR, Bray F, Forman D, Mathers C, Parkin DM. Estimates of worldwide burden of cancer in 2008: GLOBOCAN 2008. Int J Cancer 2010;127:2893–917.
2. Argiris A, Karamouzis MV, Raben D, Ferris RL. Head and neck cancer. Lancet 2008;371:1695–709.
3. Parkin DM, Bray F, Ferlay J, Pisani P. Global cancer statistics, 2002. CA Cancer J Clin 2005;55:74–108.
4. Howlader NNA, Krapcho M, Neyman N, et al., editors. SEER Cancer Statistics Review, 1975–2008. Bethesda, MD: National Cancer Institute; 2011.

5. Brizel DM, Albers ME, Fisher SR, Scher RL, Richtsmeier WJ, Hars V, et al. Hyperfractionated irradiation with or without concurrent chemotherapy for locally advanced head and neck cancer. N Engl J Med 1998;338:1798–804.
6. Brizel DM, Esclamado R. Concurrent chemoradiotherapy for locally advanced, nonmetastatic, squamous carcinoma of the head and neck: consensus, controversy, and conundrum. J Clin Oncol 2006;24:2612–7.
7. Salama JK, Seiwert TY, Vokes EE. Chemoradiotherapy for locally advanced head and neck cancer. J Clin Oncol 2007;25:4118–26.
8. Forastiere AA, Goepfert H, Maor M, Pajak TF, Weber R, Morrison W, et al. Concurrent chemotherapy and radiotherapy for organ preservation in advanced laryngeal cancer. N Engl J Med 2003;349:2091–8.
9. Jeremic B, Shibamoto Y, Milicic B, Nikolic N, Dagovic A, Aleksandrovic J, et al. Hyperfractionated radiation therapy with or without concurrent low-dose daily cisplatin in locally advanced squamous cell carcinoma of the head and neck: a prospective randomized trial. J Clin Oncol 2000;18:1458–64.
10. Cooper JS, Pajak TF, Forastiere AA, Jacobs J, Campbell BH, Saxman SB, et al. Postoperative concurrent radiotherapy and chemotherapy for high-risk squamous-cell carcinoma of the head and neck. N Engl J Med 2004;350:1937–44.
11. Calais G, Alfonsi M, Bardet E, Sire C, Germain T, Berqerot P, et al. Randomized trial of radiation therapy versus concomitant chemotherapy and radiation therapy for advanced-stage oropharynx carcinoma. J Natl Cancer Inst 1999;91:2081–6.
12. Genden EM, Ferlito A, Bradley PJ, Rinaldo A, Scully C. Neck disease and distant metastases. Oral Oncol 2003;39:207–12.
13. Suda T, Tsunoda T, Daigo Y, Nakamura Y, Tahara H. Identification of human leukocyte antigen-A24-restricted epitope peptides derived from gene products upregulated in lung and esophageal cancers as novel targets for immunotherapy. Cancer Sci 2007;98:1803–8.
14. Kono K, Mizukami Y, Daigo Y, Takano A, Masuda K, Yoshida K, et al. Vaccination with multiple peptides derived from novel cancer–testis antigens can induce specific T-cell responses and clinical responses in advanced esophageal cancer. Cancer Sci 2009;100:1502–9.
15. Yamabuki T, Daigo Y, Kato T, Hayama S, Tsunoda T, Miyamoto M, et al. Genome-wide gene expression profile analysis of esophageal squamous cell carcinomas. Int J Oncol 2006;28:1375–84.
16. Ishikawa N, Takano A, Yasui W, Inai K, Nishimura H, Ito H, et al. Cancer–testis antigen lymphocyte antigen 6 complex locus K is a serologic biomarker and a therapeutic target for lung and esophageal carcinomas. Cancer Res 2007;67:11601–11.
17. Date Y, Kimura A, Kato H, Sasazuki T. DNA typing of the HLA-A gene: population study and identification of four new alleles in Japanese. Tissue Antigens 1996;47:93–101.
18. Ohmori M, Yasunaga S, Maehara Y, Sugimachi K, Sasazuki T. DNA typing of HLA class I (HLA-A) and class II genes (HLA-DR, -DQ and -DP) in Japanese patients with gastric cancer. Tissue Antigens 1997;50:277–82.
19. Kono K, Iinuma H, Akutsu Y, Tanaka H, Hayashi N, Uchikado Y, et al. Multicenter, phase II clinical trial of cancer vaccination for advanced esophageal cancer with three peptides derived from novel cancer–testis antigens. J Transl Med 2012;10:141–9.
20. CLIA.; Available from https://www.cms.gov/CLIA/05_CLIA_Brochures.asp.
21. ICH.; Available from http://www.ich.org/products/guidelines.html
22. Vormorken JB, Psyrri A, Mesia R, Peyrade F, Beier F, de Blas B, et al. Impact of tumor HPV status on outcome in patients with recurrent and/or metastatic squamous cell carcinoma of the head and neck receiving chemotherapy with or without cetuximab: retrospective analysis of the phase III EXTREME trial. Ann Oncol 2014:25:801–7.
23. Psyrri A, Rampias T, Vermorken JB. The current and future impact of human papillomavirus on treatment of squamous cell carcinoma of the head and neck. Ann Oncol 2014;25:2101–15.
24. Kantoff PW, Higano CS, Shore ND, Berger ER, Small EJ, Penson DF, et al. Impact study investigators. Sipuleucel-T immunotherapy for castration-resistant prostate cancer. N Engl J Med 2010;363:411–22.
25. Weber JS, O'Day S, Urba W, Powderly J, Nichol G, Yellin M, et al. Phase I/II study of ipilimumab for patients with metastatic melanoma. J Clin Oncol 2008;26:5950–6.
26. Schwartzentruber DJ, Lawson DH, Richards JM, Conry RM, Miller DM, Treisman J, et al. gp100 peptide vaccine and interleukin-2 in patients with advanced melanoma. N Engl J Med 2011;364:2119–27.
27. Schuster SJ, Neelapu SS, Gause BL, Janik JE, Muggia FM, Gockerman JP, et al. Vaccination with patient-specific tumor-derived antigen in first remission improves disease-free survival in follicular lymphoma. J Clin Oncol 2011;29:2787–94.
28. Cecco S, Muraro E, Giacomin E, Martorelli D, Lazzarini R, Baldo P, et al. Cancer vaccines in phase II/III clinical trials: state of the art and future perspectives. Curr Cancer Drug Targets 2011;11:85–102.
29. Noguchi M, Moriya F, Suekane S, Matsuoka K, Arai G, Matsueda S, et al. Phase II study of personalized peptide vaccination for castration-resistant prostate cancer patients who failed in docetaxel-based chemotherapy. Prostate 2012;72:834–45.
30. Slingluff CL Jr, Petroni GR, Chianese-Bullock KA, Smolkin ME, Ross MI, Haas NB, et al. Randomized multicenter trial of the effects of melanoma-associated helper peptides and cyclophosphamide on the immunogenicity of a multipeptide melanoma vaccine. J Clin Oncol 2011;29:2924–32.
31. Lutz E, Yeo CJ, Lillemoe KD, Biedrzycki B, Kobrin B, Herman J, et al. A lethally irradiated allogeneic granulocyte-macrophage colony stimulating factor-secreting tumor vaccine for pancreatic adenocarcinoma. A Phase II trial of safety, efficacy, and immune activation. Ann Surg 2011;253:328–35.
32. Okada H, Kalinski P, Ueda R, Hoji A, Kohanbash G, Donegan TE, et al. Induction of CD8+ T-cell responses against novel glioma-associated antigen peptides and clinical activity by vaccinations with {alpha}-type 1 polarized dendritic cells and polyinosinic-polycytidylic acid stabilized by lysine and carboxymethylcellulose in patients with recurrent malignant glioma. J Clin Oncol 2011;29:330–6.
33. Lesterhuis WJ, Haanen JB, Punt CJ. Cancer immunotherapy–revisited. Nat Rev Drug Discov 2011;10:591–600.
34. Vikesaa J, Hansen TV, Jùnson L, Borup R, Wewer UM, Christiansen J, et al. RNA-binding IMPs promote cell adhesion and invadopodia formation. EMBO J 2006;25:1456–68.
35. de Cárcer G, Pérez de Castro I, Malumbres M. Targeting cell cycle kinases for cancer therapy. Curr Med Chem 2007;14:969–85.
36. Mizukami Y, Kono K, Daigo Y, Takano A, Tsunoda T, Kawaguchi Y, et al. Detection of novel cancer–testis antigen-specific T-cell responses in TIL, regional lymph nodes, and PBL in patients with esophageal squamous cell carcinoma. Cancer Sci 2008;99:1448–54.
37. Germeau C, Ma W, Schiavetti F, Lurquin C, Henry E, Vigneron N, et al. High frequency of antitumor T cells in the blood of melanoma patients before and after vaccination with tumor antigens. J Exp Med 2005;201:241–8.
38. Keilholz U, Weber J, Finke JH, Gabrilovich DI, Kast WM, Disis ML, et al. Immunologic monitoring of cancer vaccine therapy: results of a workshop sponsored by the society for biological therapy. J Immunother 2002;25:97–138.
39. Butterfield LH, Palucka AK, Britten CM, Dhodapkar MV, Håkansson L, Janetzki S, et al. Recommendations from the iSBTc-SITC/FDA/NCI workshop on immunotherapy biomarkers. Clin Cancer Res 2011;17:3064–76.
40. Bedognetti D, Balwit JM, Wang E, Disis ML, Britten CM, Delogu LG, et al. SITC/iSBTc cancer immunotherapy biomarkers resource document: online resources and useful tools - a compass in the land of biomarker discovery. J Transl Med 2011;9:155.
41. Sawada Y, Yoshikawa T, Nobuoka D, Shirakawa H, Kuronuma T, Motomura Y, et al. Phase I trial of a glypican-3-derived peptide vaccine for advanced hepatocellular carcinoma: immunologic evidence and potential for improving overall survival. Clin Cancer Res 2012;18:3686–96.
42. Tomita Y, Yuno A, Tsukamoto H, Senju S, Kuroda Y, Hirayama M, et al. Identification of promiscuous KIF20A long peptides bearing both $CD4^+$ and $CD8^+$ T-cell epitopes: KIF20A-specific $CD4^+$ T-cell immunity in patients with malignant tumor. Clin Cancer Res 2013;19:4508–20.
43. Tomita Y, Yuno A, Tsukamoto H, Senju S, Yoshimura S, Osawa R, et al. Identification of CDCA1-derived long peptides bearing both $CD4^+$ and $CD8^+$ T-cell epitopes: CDCA1-specific $CD4^+$ T-cell immunity in cancer patients. Int J Cancer 2013;134:352–66.
44. Hailemichael Y, Dai Z, Jaffarzad N, Ye Y, Medina MA, Huang XF, et al. Persistent antigen at vaccination sites induces tumor-specific $CD8^+$ T cell sequestration, dysfunction and deletion. Nat Med 2013;19:465–72.

IJC
International Journal of Cancer

Analysis of circulating tumor cells derived from advanced gastric cancer

Kosei Toyoshima[1], Akira Hayashi[1], Masahide Kashiwagi[1], Naoko Hayashi[2], Masaaki Iwatsuki[2], Takatsugu Ishimoto[2], Yoshifumi Baba[2], Hideo Baba[2] and Yoshikazu Ohta[1]

[1] Oncology Drug Discovery Unit, Pharmaceutical Research Division, Takeda Pharmaceutical Company Limited, Fujisawa, Kanagawa, 251-8555, Japan
[2] Department of Gastroenterological Surgery, Graduate School of Medical Sciences, Kumamoto University, Kumamoto, Kumamoto, 860-0811, Japan

Studies in circulating tumor cells (CTCs) have proceeded to be accepted as prognostic markers in several types of cancers. But they are still limited because many are mainly from enumeration of CTCs. Here, we tried to evaluate the tumorigenicity of CTCs from advanced gastric cancer patients ($n = 42$). Peripheral blood mononuclear cells (PBMC) from the patients were separated into CD45 negative and positive fractions and both were subcutaneously injected into immunodeficient mice. Within 5 months nine tumor-like-structures from six patients but not from healthy volunteers were established. They were durable for passages and all had been confirmed human origin. Eight of the nine tumor-like-structures were from nonauthorized CTC containing cells expressing CD45 and B-cell markers. On the contrary, one of them was developed from $CD45^-$ PBMC fraction of a patient with bone marrow metastasis reflecting authorized CTCs. Histopathology showed common features with that of original gastric tumor. The cells isolated from the tumor-like-structure expressed EpCAM and CEA further supporting they were from the original tumor. Moreover the cells were CD44 positive to varying degree and a limiting dilution study showed that the $CD44^{+/high}$ fraction had tumorigenicity. The CD44 was dominantly in the form of CD44 variant 8–10. The $CD44^{+/high}$ cells had higher expression of the glutamate/cysteine transporter xCT compared with the $CD44^{-/low}$ cells. Our results showed the existence of tumor-initiating cells in blood of advanced gastric cancer patients and they could be a therapeutic target and prospective tool for further investigations.

Gastric cancer is one of the most common digestive malignancies worldwide.[1] Despite improvement in diagnostics and therapeutics, signet-ring cell carcinomas and poorly differentiated adenocarcinomas are known as the mortal types of gastric cancer reflecting their propensity for metastases.[2,3] One of the most common metastatic sites is a liver. The 5-year survival rate of gastric cancer patients with liver metastasis is 34% even if they underwent hepatic resection.[4] Compared to them, the bone marrow metastasis is quite rare, but it tends to provoke fatal hematological disorders such as disseminated intravascular coagulation and shows shorter survival.[5]

Circulating tumor cells (CTCs) are detected in the peripheral blood of metastatic cancer patients. Numerous clinical studies with the CellSearch system® have demonstrated the utility of CTC as a biomarker.[6] However, the molecular and biological properties of CTCs are still to be elucidated only with a few reports of genomic and proteomic characteristics.[7] Just recently, some reports showed tumorigenicity of CTCs.[8–10]

The present study shows that tumor-initiating cells are present in the peripheral blood of advanced gastric cancer patients through the establishment of *in vivo* transplantable tumors in mice from patient CTCs. These CTC could be a therapeutic target. The tumor obtained can be used to further examine the biological characteristics of CTCs.

Key words: circulating tumor cells, gastric cancer, CD44, tumorigenicity
Additional Supporting Information may be found in the online version of this article.
Grant sponsor: Grant sponsor: Takeda Pharmaceutical Company Limited [K.T., A.H., M.K. and Y.O (employees) and N.H., M.I., T.I., Y.B. and H.B]
DOI: 10.1002/ijc.29455
History: Received 25 Nov 2014; Accepted 2 Jan 2015; Online 27 Jan 2015
Correspondence to: Kosei Toyoshima, Oncology Drug Discovery Unit, Pharmaceutical Research Division, Takeda Pharmaceutical Company Limited, 26-1 Muraoka-Higashi 2-chome, Fujisawa, Kanagawa 251-8555, Japan, Fax: +81-466-29-4412, E-mail: kousei.toyoshima@takeda.com

Methods

Patient enrollment and CTC count procedures

The study protocol was approved by the ethics committee of Kumamoto University. Forty-two gastric cancer patients were enrolled, and informed consent was obtained from all patients. Peripheral blood (5–15 ml) samples were collected from the patients in heparin blood collection tubes from 1 to 15 times during the treatment period. The number of CTCs per 7.5 ml of blood was enumerated using a CellSearch system® (Veridex LLC), according to the manufacturer's instructions.

Short Report

What's new?
Circulating tumor cells (CTCs) are found in the peripheral blood of metastatic cancer patients, and may offer prognostic biomarkers for several types of cancer. In this study, the authors evaluated whether CTCs from advanced gastric cancer patients are actually tumorigenic. Injecting peripheral blood mononuclear cells (PBMCs) from these patients into mice produced tumors, while PBMCs from healthy volunteers did not. CTCs from gastric cancer patients may thus offer a potential therapeutic target, as well as a tool for further investigation.

Tumor establishment from PBMC of the cancer patients

Mice experiments and housing procedures were performed under the approval of Takeda's animal study committee, which recently acquired AAALAC accreditation. Female NOD/SCID mice (age, 5 weeks) were purchased from Charles River Japan. The mice were treated with anti-mouse CD122 antibody (553359, BD) to suppress natural killer cells.[11]

Patients' peripheral blood mononuclear cells (PBMC) were isolated using Lymphoprep® (1114544, Axis-Shield). PBMC were enriched for CTCs using Whole Blood CD45 MicroBeads (130-090-872, Miltenyi Biotec). $CD45^+$ or $CD45^-$ fraction was inoculated subcutaneously into the immunodeficient mice. Each fraction was transplanted to an individual mouse, respectively. For passage, the established tumor-like-structures were cut into small pieces of approximately 2^3 mm^3 and were subcutaneously inoculated into recipient immunodeficient mice.

Flow cytometric analysis and cell sorting

Tumor-like-structures were cut into small pieces and minced thoroughly using sterile blades. To obtain single cell suspensions, the minced tumors were mixed with Accutase™ (AT-104, Innovative Cell Technologies) and incubated at 37 °C for 2 hr with pipetting every 20–25 min. Subsequently, the cells were filtered through a 100-μm nylon mesh and dead cells were separated using a dead cell removal kit (130-090-101, Miltenyi Biotec). Dead cells were further excluded by PI staining. Live cells were stained with the following anti-human antibodies: CD19-FITC (ab1167, Abcam), CD20-FITC (ab46895, Abcam), CD40-FITC (ab27281, Abcam), CD44 -FITC (ab18243, Abcam), CD45-FITC (130-080-202, Miltenyi Biotec), CD133-PE (130-080-801, Miltenyi Biotec), CEA-FITC (ab46538, Abcam), EpCAM-FITC (130-080-301, Miltenyi Biotec) and HLA Class 1-PE (ab58998, Abcam). Labeled cells were analyzed using FACSVantage™ or FACSAria™ (BD). HLA^+ cells were sorted into $CD44^{+/high}$ and $CD44^{-/low}$ fractions using FACSAria and used for other assays.

Limiting dilution assay

The sorted $CD44^{+/high}$ and $CD44^{-/low}$ cells were suspended in a 1:1 mixture of serum-free RPMI 1640 (22400-089, Life Technologies) and Matrigel (growth factor reduced, 356231, BD), and injected subcutaneously on two sides of each mouse. Thereafter, tumor size was measured using calipers, and volumes were calculated using the following formula: (large diameter) × (small diameter)^2/2.

RNA isolation and cDNA synthesis

Total RNA was extracted from tumor-like-structures using an RNeasy Lipid Tissue Mini Kit (74804, Qiagen), according to the manufacturer's instructions and quantified using a NanoDrop 1000 spectrophotometer (Thermo Scientific). Subsequently, cDNA was synthesized using a SuperScript® VILO™ cDNA Synthesis Kit (11754-050, Life Technologies).

RT-PCR

Semiquantitative RT-PCR analysis was performed using the following human primer sets: CD44 forward, 5′-TCCCAGACGAAGACAGTCCCTGGAT-3′ and reverse 5′-CACTGGGGTGGAATGTGTCTTGGTC-3′ and β-actin (ACTB), TaqMan probe set Hs99999903_m1. PCR conditions were as follows: 10 min at 95 °C, followed by 30 cycles of 95 °C for 30 sec, 60 °C for 30 sec, and 72 °C for 45 sec, with a final extension for 7 min at 72 °C. Quantitative RT-PCR was performed using an ABI PRISM® 7900HT system (Applied Biosystems). The following TaqMan probes were used: CD44, Hs00174139_m1; SLC7A11, Hs00921938_m1; ACTB (internal control), Hs99999903_m1 and human GAPDH (4326317E, Applied Biosystems). PCR conditions were as follows: 10 min at 95 °C, followed by 40 cycles of 95 °C for 15 sec, 60 °C for 60 sec. Expression values were calculated relative to ACTB (the endogenous control) using the ΔΔCT algorithm.

Histopathology

Samples were fixed in 4% paraformaldehyde phosphate buffer solution (163-20145, Wako) and embedded in paraffin. The specimens were sliced into 5-μm-thick and stained with hematoxylin and eosin (H&E). For immunohistochemistry, antigens were retrieved in sodium citrate buffer (pH = 6.0) by microwave. After blocking, the sections were incubated with a monoclonal rabbit anti-EpCAM antibody (ab124825, 1:200, Abcam) and anti-CD20 antibody (ab78237, 1:1,000, Abcam) overnight at 4 °C. Staining was developed using DAB solution (K3468, Dako) and counterstained with hematoxylin.

EB virus detection

RNA extraction from tumor-like-structures and EB virus detection were conducted in ScyMed Incorporated (Tokyo,

Japan). EB virus was detected by quantitative RT-PCR for BFRF-3 gene.

Results

CTCs in advanced gastric cancer patients

Forty-two gastric cancer patients with Stage IV (29 patients) or recurrence (13 patients) and 15 healthy volunteers were prospectively recruited for the present study. The patient information was summarized in Table 1. CTCs were detected in 28 of the 42 (66.7%) patients. In the Stage IV patients, 17 (58.6%) had CTCs. In the recurrence patients, 11 (84.6%) had CTCs. According to previous reports, distant metastases are one of the most important factors to detect CTCs.[12–14] In this study, 23 (54.8%) patients had distant metastases and CTCs were detected in 17 of the 23 (73.9%) patients. Whereas 19 (45.2%) patients were without distant metastases, and 11 of the 19 (57.9%) had CTCs. Among the patients with distant metastases, seven patients had bone metastasis and 14 patients had peritoneal dissemination. CTCs were detected in six of the seven (85.7%) and 10 of the 14 (71.4%) patients, respectively. Three of the seven patients with bone metastasis had CTCs more than several thousand. CTCs were not identified in the blood samples from healthy volunteers.

Tumor-like-structure was established from PBMC of advanced gastric cancer patients

We investigated whether tumor initiating cells are contained in PBMC of advanced gastric cancer patients. Because CTCs are defined as $EpCAM^+/CD45^-$ nucleated cells in CellSearch system®, the $CD45^-$ fractions of PBMC were injected subcutaneously into immunodeficient mice. As a control, $CD45^+$ fractions were also inoculated. Within 5 months, detectable tumor-like-structures (>50 mm^3) were established in nine samples from six patients (Table 1). Contrary to our expectation, eight of the nine tumor-like-structures were developed from $CD45^+$ fractions whereas one of them was developed from $CD45^-$ fraction.

Of the six patients, patient #11 was diagnosed as Stage IV signet-ring cell carcinoma with multiple bone marrow metastases and underwent chemotherapy. Bone metastases were detected by whole body bone scintigraphy (unpublished data). This patient had 0–18,015 CTCs/7.5 ml of blood detected by the CellSearch system®. The number of CTCs was varied depending on the chemotherapy. PBMC from the patient #11 developed three tumor-like-structures. One of them was developed from the $CD45^-$ fraction. The others were developed from the $CD45^+$ fraction. Patient #13 was diagnosed as recurrence and bone marrow metastasis and underwent chemotherapy. This patient had 201–7,433 CTCs/7.5 ml of blood. $CD45^+$ fraction from the patient #13 developed two tumor-like-structures. Patient #22 was diagnosed as Stage IV without distant metastases and underwent chemotherapy. This patient had 3–12 CTCs/7.5 ml of blood. The $CD45^+$ fraction, which was derived from the blood sample donated on the next day of bypass surgery, developed a tumor-like-structure. Patient #19, #20 and #23 were diagnosed as Stage IV without distant metastases and did not undergo any treatment or surgery. Although CTCs from these patients were not detected by CellSearch system®, their $CD45^+$ fractions developed tumor-like-structures. Of note, peripheral blood samples from 15 healthy volunteers did not give rise to any tumor-like-structures even 6 months after injection.

Analysis of the established tumor-like-structures

To evaluate whether or not the established tumor-like-structures were derived from CTCs, we checked they were human origin. Human GAPDH expression was measured by RT-qPCR and surface markers by a flow cytometer on cells isolated from the nine established tumor-like-structures. In all the human GAPDH (data not shown) were detected and all isolated cells were positively stained with anti-hu-HLA antibody, indicating that they were derived from human cells. The human cells isolated from eight of the nine tumor-like-structures expressed B-cell markers such as CD45, CD19 and CD20 but not EpCAM (Supporting Information Fig. 1). Moreover, Epstein–Barr virus (EBV) infection was confirmed in these cells. These tumor-like-structures were durable for the subcutaneous passage in immunodeficient mice.

On the contrary, one tumor-like-structure was developed from the $CD45^-$ fraction of the patient #11 (Fig. 1*a*). It was predominantly tubular adenocarcinomas, with a smaller number of signet-ring cells (Fig. 1*b*). This tumor was also durable for passage and the secondary transplant included signet-ring cells as well (Fig. 1*c*). On the other hand, original patient tumors were poorly cohesive carcinomas of signet-ring cells (Fig. 1*d*). Although tumor differentiation did not correspond completely, signet-ring cell carcinomas were common to both original patient and xenograft tumors. The established tumor was developed by EpCAM expressing cells, not stained with CD45 and CD20 antibody (Figs. 1*e–g*). It was not infected by EBV. These cells were CEA^+, indicating that they were gastrointestinal tumor origin.[15]

The sample which developed the tumor was taken when the patient #11 became refractory to the treatment. CTC-enriched $CD45^-$ fraction including 4×10^3 CTCs were injected into an immunodeficient mouse and formed tumor by Day 37 after inoculation. Furthermore CTCs were detected in the peripheral blood of passaged tumor-bearing mice using the CellSearch system® (data not shown).

CD44-expressing cells play a central role for the tumorgenesis

The cells isolated from the tumor established from the $CD45^-$ fraction were further analyzed. Importantly, they were $CD44^+$ to varying degrees (Fig. 1*e*). Because CD44 has been used as a CSC marker in several cancers including gastric cancer,[16,17] we confirmed the relationship between tumorigenicity and CD44 expression. To investigate tumorigenicity, $CD44^{+/high}$ and $CD44^{-/low}$ fractions were sorted out and 100–10,000 cells of each fraction were inoculated into

Short Report

Table 1. Summary of the gastric cancer patients enrolled

No.	Sex	Age	Major distant metastasis	Stage*	Status at the blood sampling	Range of CTCs (per 7.5mL, CellSearch)	Transplantation**
1	M	49	Multiple bone	IV	Post-chemo	0	–
2	M	59	–	IV	Pre-chemo	3–36	–
3	M	65	–	IV	Pre-chemo	7	–
4	M	62	Lung	IV	Pre-chemo	0	–
5	F	42	Peritoneal dissemination	Rec	Pre-chemo	2–27	–
6	M	42	–	IV	Post-chemo	4–44	–
7	M	63	–	IV	Pre-chemo	8	–
8	M	58	–	IV	Pre-chemo	14	–
9	F	43	–	IV	Post-chemo	60	–
10	F	81	–	IV	Pre-chemo	0	–
11	F	44	Bone marrow	IV	Post-chemo	0–18,015	○
12	F	31	Carcinomatous lymphangiosis	IV	Post-chemo	2–96	×
13	F	44	Bone marrow	Rec	Post-chemo	201–7,433	○
14	F	56	Multiple bone	IV	Pre-chemo	65–4,088	×
15	F	58	Bone marrow	Rec	Pre-chemo	30–42	×
16	M	61	–	IV	Pre-chemo	19	×
17	M	62	–	IV	Pre-chemo	9	×
18	F	58	–	IV	Pre-chemo	4	×
19	M	61	–	IV	Pre-chemo	0	○
20	M	82	–	IV	Pre-chemo	0	○
21	M	56	–	IV	Pre-chemo	0	×
22	M	46	–	IV	Post-chemo	3–12	○
23	M	60	–	IV	Pre-chemo	0	○
24	F	51	–	Rec	Post-chemo	0	×
25	M	55	Peritoneal dissemination	Rec	Pre-chemo	44	×
26	M	77	suspected peritoneal dissemination	Rec	Post-surgery	125	×
27	M	83	–	Rec	Post-surgery	1	×
28	M	63	suspected peritoneal dissemination	Rec	Post-surgery	97	×
29	M	27	Bone marrow	IV	Pre-chemo	98	×
30	M	80	–	IV	Pre-chemo	0	×
31	M	27	Bone marrow	IV	Post-chemo	93 - 261	×
32	M	49	Peritoneal dissemination	IV	Pre-chemo	0	×
33	F	59	Peritoneal dissemination	Rec	Post-chemo	15	×
34	M	70	Peritoneal dissemination	IV	Pre-chemo	8	×
35	F	59	Peritoneal dissemination	Rec	Post-chemo	7	×
36	M	69	Peritoneal dissemination	IV	Pre-chemo	0	×
37	M	49	Peritoneal dissemination	IV	Post-chemo	0	×
38	M	53	Peritoneal dissemination	Rec	Post-chemo	14	×
39	M	53	Peritoneal dissemination	Rec	Post-chemo	32	×
40	M	71	Peritoneal dissemination, Liver	IV	Post-chemo	26	×
41	M	62	–	IV	Pre-surgery	0	×
42	M	47	Peritoneal dissemination	Rec	Pre-chemo	0	×

*Rec: Recurrence, **-: Nontransplantation, ○: Tumor-like-structure formation, ×: Nontumor-like-structure formation.

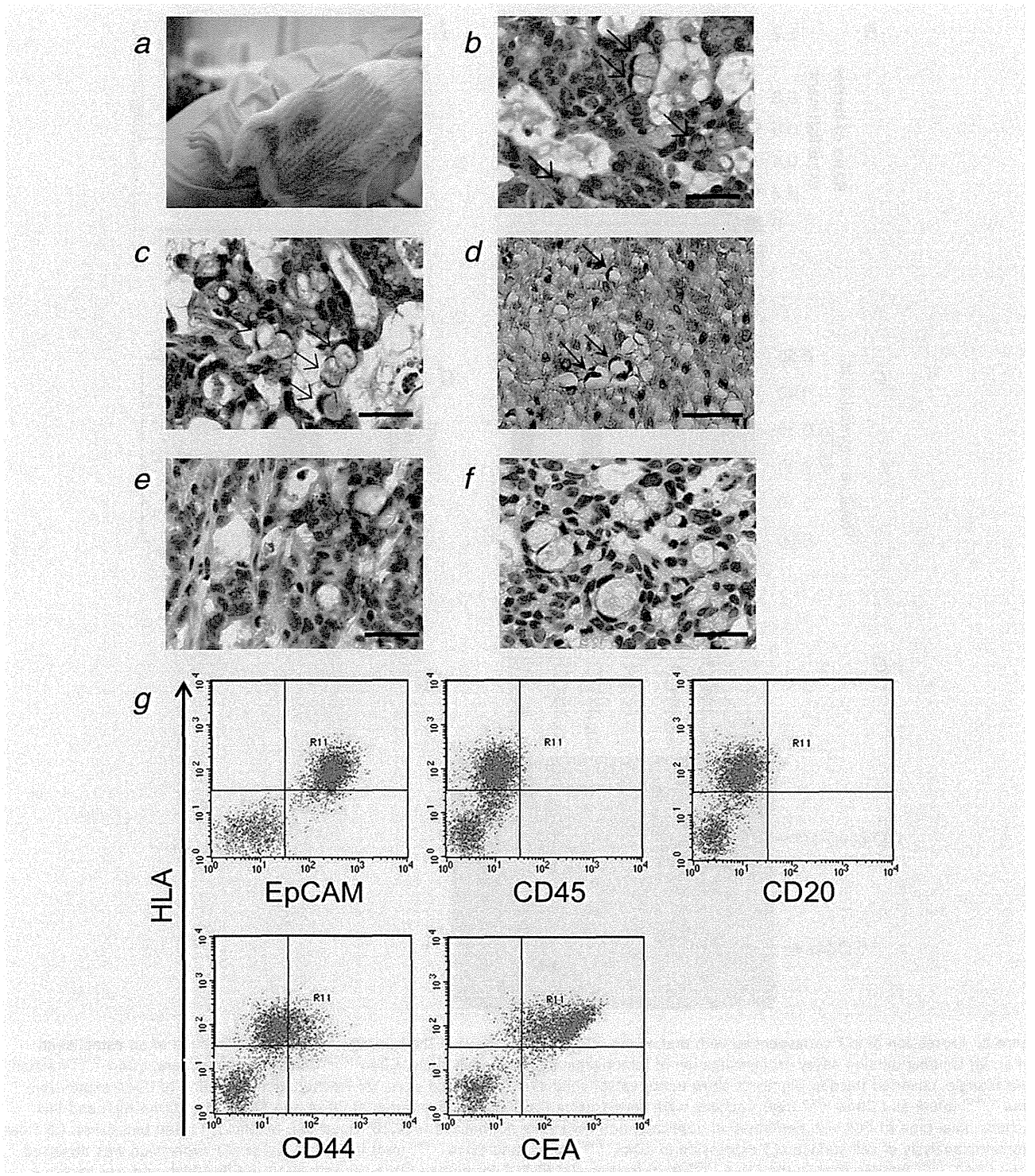

Figure 1. A tumor established from PBMC of gastric cancer patients (*a*) $CD45^-$ fraction was subcutaneously injected abdomen of immunodeficient mouse. Tumor (passage 0) was developed in 37 days. (*b, c*) H&E staining of FFPE sample from established tumor containing signet-ring cells. Arrows show signet-ring cells. Scale bar shows 25 μm. (*b*) First xenografted tumor. (*c*) Secondary xenografted tumor. (*d*) H&E staining of FFPE samples from original tumors showing a signet-ring cell carcinoma. Arrows shows signet-ring cells. Scale bar shows 30 μm. (*e*) EpCAM staining of the established tumor. Brown: EpCAM. Blue: nucleus. (*f*) CD20 staining of the established tumor. Brown: CD20. Blue: nucleus. (*g*) A tumor-like-structure from $CD45^-$ fraction was dissociated into single cells and stained with anti-HLA antibody and each antibody described for an analysis by FACSAria. HLA^+ cells were $EpCAM^+/CD45^-$ matched with CTCs. They also expressed the marker of gastrointestinal cancer, CEA, but not B cell markers. They expressed CD44 to varying degree.

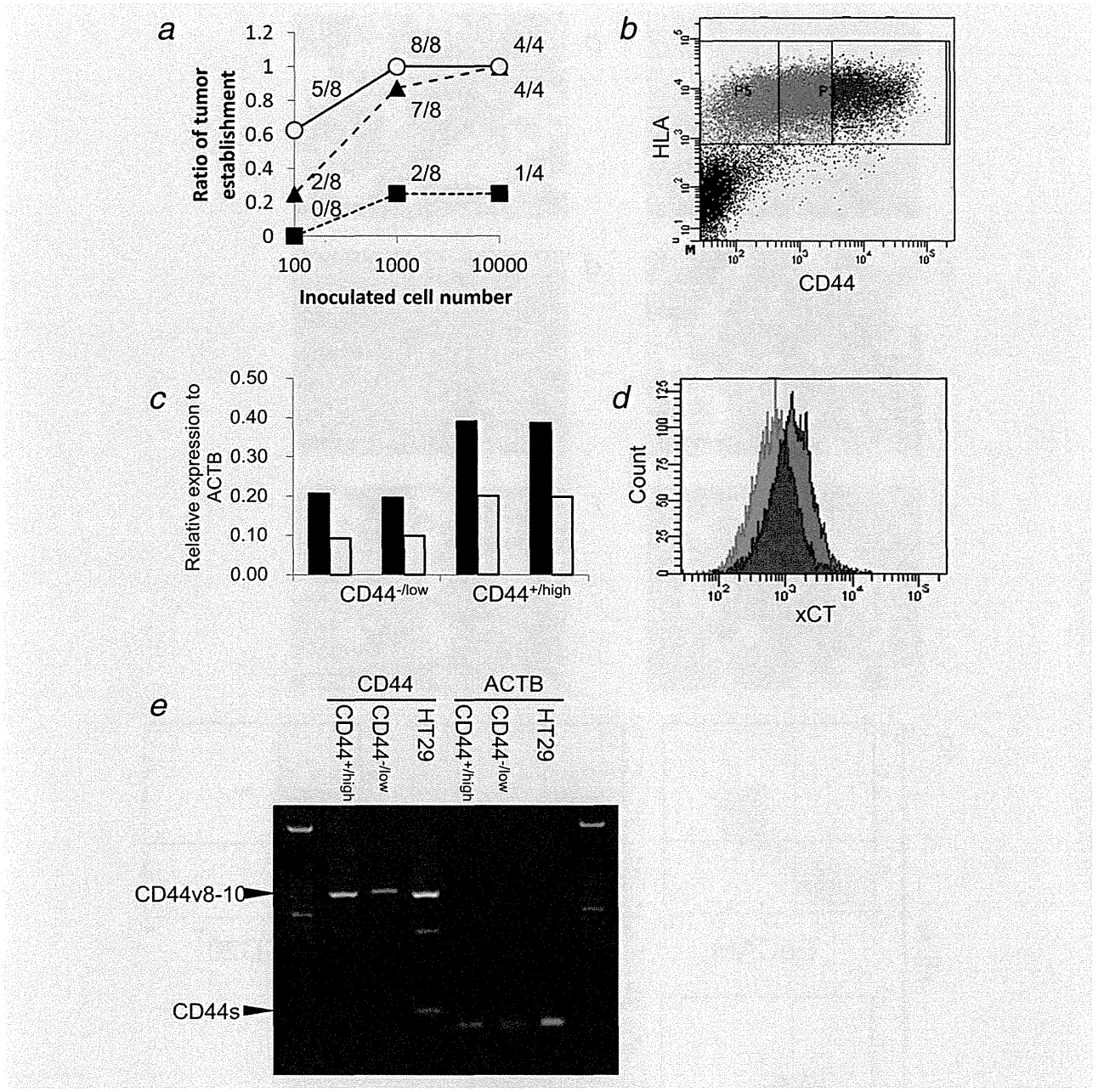

Figure 2. Expression of xCT corresponded with that of the CD44 variants 8–10 in the tumorigenic $CD44^{+/high}$ fraction of an established tumor. (*a*) Limiting dilution assay for investigation of tumorigenic fraction; open circle, $CD44^{+/high}$ fraction; solid square, $CD44^{-/low}$ fraction; solid triangle, unsorted fraction. Numbers show tumor established sites/inoculated sites. (*b*) Fractionation according to CD44 expression; $CD44^{+/high}$ (blue) and $CD44^{-/low}$ (red) fractions were sorted using FACSAria. (*c*) Expression of CD44 and SLC7A11 in CD44 high and low fractions. Real time RT-PCR was performed in duplicate, and data were normalized to ACTB; Open bar, SLC7A11; Closed bar, CD44. (*d*) Flow cytometric analysis of cell surface xCT expression in $CD44^{+/high}$ (blue) and $CD44^{-/low}$ (red) fractions. Higher xCT expression was observed in the $CD44^{+/high}$ fraction than in the $CD44^{-/low}$ (red) fraction. (*e*) RT-PCR for human CD44 variants 8–10 in CD44 high and low fractions. The $CD44^{+/high}$ fraction had high expression of CD44 variants 8–10. HT29 cells were used as a positive control.[18]

Short Report

immunodeficient mice. The $CD44^{+/high}$ fraction gave rise to detectable tumors (>50 mm^3) even from only 100 cells, whereas the $CD44^{-/low}$ fraction was not tumorigenic (Fig. 2*a*). These observations strongly indicate that $CD44^{+/high}$ cells are tumor-initiating cells.

The tumor cells were separated into $CD44^{+/high}$ (blue) and $CD44^{-/low}$ (red) fractions (Fig. 2*b*), and the expression of xCT/SLC7A11 in each fraction was confirmed by RT-qPCR and FACS analyses (Figs. 2*cd*). In both assays, the $CD44^{+/high}$ cells expressed higher levels of xCT/SLC7A11

than the $CD44^{-/low}$ cells. Of note, the CD44 variants 8–10 showed dominant expression in both fractions (Fig. 2*e*).

Discussion

For the main purpose of the present study, a functional analysis of CTC, we enrolled the advanced gastric cancer patients (Stage IV and recurrence) predicting larger number of CTCs in them. Although a statistical discussion about the CTC number may have limited meaning, we could elicit three tendencies from our study. First, as we expected,[19] CTC positive ratio was high in the advanced patients especially in the recurrence, most of whom were CTC positive. Second, CTC positive ratio of the patients without distant metastases was higher than previous report.[20] The reason might be that the patients had lateral metastases.[21] Third, the patients with bone metastasis tended to have higher CTCs positive ratio and CTC number than those of the patients with peritoneal dissemination. This result might be accordance with that peritoneal dissemination is not hematogenous metastasis. It has been thought that hematogenous metastases, especially bone metastasis, might be one of key factors for CTC detection.[6]

We here captured CTCs by directly injecting them into immunodeficient mice and established and passaged tumor lines for further biological analyses. We believe our data demonstrate the tumorigenicity of CTCs. A tumor tissue grew after the subcutaneous injection of $CD45^{-}$ cells into an immunodeficient mouse, and the established tumors included signet-ring cell carcinomas representing the original patient tumors. Furthermore, they comprised predominantly of $EpCAM^{+}/CD45^{-}$ cells (Fig. 1*e*).

We confirmed that CD44 positive cells have a strong tumorgenecity. The xCT expression was upregulated in the $CD44^{+/high}$ fraction. The CD44 variant 8–10 was dominantly expressed in the human cells from the tumor (Fig. 2*e*). These results suggested that CSCs were present in the $CD44^{+/high}$ fraction. Previous data showed that CD44 variants 8–10 stabilized xCT and that this interaction contributed to the maintenance of CSC populations.[18]

To date, only a few studies have shown tumorigenicity of CTCs.[8–10] In 2 of them,[8,9] desired fraction of the cells was inoculated after cultivation. And the model of Baccelli *et al.* took 6–12 months before developping metastatic growth.[10] Our present study provided another case to show potent tumorgenecisy of CTCs, which could be a therapeutic target. It may reflect the the clinical severity of the donnar patient (unpublished data) or the number of the cells with CSCs prevalence.[22] These cellular information and the established cell lines, with more cases accumulated, would facilitate the future study of CTC or cancer therapy.

We also established tumor-like-structures containing the cells expressing B cell markers and infected by EBV. EBV-associated B-cell lymphomas have been reported in the primary human hepatocellular carcinomas xenografted into immunodeficient mice.[23] These cells may not have direct relation with the original tumor of the patients. But we are still interested in these cells considering clinical meaning or contribution to the disease. Furthermore, the existence of the non-authorized type CTC, such as EpCAM negative, will be one of the most important issues to be elucidated.

In summary, this study provides the evidence of tumorigenic cancer cells in the peripheral blood of gastric cancer patients and indicates CD44 as an appropriate marker of such cells. The established tumor would be a prospective tool for investigations of metastatic mechanisms.

ACKNOWLEDGMENT

We would like to thank Toshiyuki Nomura, Yuichi Hikichi, Osamu Nakanishi, and Syuichi Furuya for their guidance and support during the course of this work.

References

1. Parkin DM, Bray F, Ferlay J, et al. Global cancer statistics, 2002. *CA Cancer J Clin* 2005;55:74–108.
2. Kwon KJ, Shim KN, Song EM, et al. Clinicopathological characteristics and prognosis of signet ring cell carcinoma of the stomach. *Gastric Cancer* 2014;17:43–53.
3. Kim HM, Pak KH, Chung MJ, et al. Early gastric cancer of signet ring cell carcinoma is more amenable to endoscopic treatment than is early gastric cancer of poorly differentiated tubular adenocarcinoma in select tumor conditions. *Surg Endosc* 2011;25:3087–93.
4. Okano K, Maeba T, Ishimura K, et al. Hepatic resection for metastatic tumors from gastric cancer. *Ann Surg* 2002;235:86–91.
5. Tokar M, Bobilev D, Ariad S, et al. Disseminated intravascular coagulation at presentation of advanced gastric cancer. *Isr Med Assoc J* 2006;8:853–5.
6. Miller MC, Doyle GV, Terstappen LW. Significance of circulating tumor cells detected by the CellSearch system in patients with metastatic breast colorectal and prostate cancer. *J Oncol* 2010; 2010:617421
7. Jiang Y, Palma JF, Agus DB, et al. Detection of androgen receptor mutations in circulating tumor cells in castration-resistant prostate cancer. *Clin Chem* 2010;56:1492–5.
8. Zhang L, Ridgway LD, Wetzel MD, et al. The identification and characterization of breast cancer CTCs competent for brain metastasis. *Sci Transl Med* 2013;5:180ra48
9. Chen T, Yang K, Yu J, et al. Identification and expansion of cancer stem cells in tumor tissues and peripheral blood derived from gastric adenocarcinoma patients. *Cell Res* 2012;22:248–58.
10. Baccelli I, Schneeweiss A, Riethdorf S, et al. Identification of a population of blood circulating tumor cells from breast cancer patients that initiates metastasis in a xenograft assay. *Nat Biotechnol* 2013;31:539–44.
11. Dewan MZ, Terunuma H, Takada M, et al. Role of natural killer cells in hormone-independent rapid tumor formation and spontaneous metastasis of breast cancer cells in vivo. *Breast Cancer Res Treat* 2007;104:267–75.
12. de Bono JS, Scher HI, Montgomery RB, et al. Circulating tumor cells predict survival benefit from treatment in metastatic castration-resistant prostate cancer. *Clin Cancer Res* 2008;14:6302–9.
13. Cristofanilli M, Budd GT, Ellis MJ, et al. Circulating tumor cells, disease progression, and survival in metastatic breast cancer. *N Engl J Med* 2004;351:781–91.
14. Cohen SJ, Punt CJ, Iannotti N, et al. Relationship of circulating tumor cells to tumor response, progression-free survival, and overall survival in patients with metastatic colorectal cancer. *J Clin Oncol* 2008;26:3213–21.
15. Duffy MJ, Lamerz R, Haglund C, et al. Tumor markers in colorectal cancer, gastric cancer and gastrointestinal stromal cancers: European group on tumor markers (EGTM) 2013 guidelines update. *Int J Cancer* 2014;134:2513–22.
16. Takaishi S, Okumura T, Tu S, et al. Identification of gastric cancer stem cells using the cell surface marker CD44. *Stem Cells* 2009;27:1006–20.
17. Gangopadhyay S, Nandy A, Hor P, et al. Breast cancer stem cells: a novel therapeutic target. *Clin Breast Cancer* 2013;13:7–15.
18. Ishimoto T, Nagano O, Yae T, et al. CD44 variant regulates redox status in cancer cells by stabilizing

the xCT subunit of system xc(-) and thereby promotes tumor growth. *Cancer Cell* 2011;19:387–400.
19. Uenosono Y, Arigami T, Kozono T, et al. Clinical significance of circulating tumor cells in peripheral blood from patients with gastric cancer. *Cancer* 2013;119:3984–91.
20. Muller V, Stahmann N, Riethdorf S, et al. Circulating tumor cells in breast cancer: correlation to bone marrow micrometastases, heterogeneous response to systemic therapy and low proliferative activity. *Clin Cancer Res* 2005;11:3678–85.
21. Hristozova T, Konschak R, Stromberger C, et al. The presence of circulating tumor cells (CTCs) correlates with lymph node metastasis in nonresectable squamous cell carcinoma of the head and neck region (SCCHN). *Ann Oncol* 2011;22:1878–85.
22. Al-Hajj M, Wicha MS, Benito-Hernandez A, Morrison SJ, Clarke. Prospective identification of tumorigenic breast cancer cells. *Proc Natl Acad Sci USA* 2003;100:3983–8.
23. Chen K, Ahmed S, Adeyi O, et al. Human solid tumor xenografts in immunodeficient mice are vulnerable to lymphomagenesis associated with Epstein-barr virus. *PloS One* 2012;7:e39294

J Gastroenterol (2014) 49:1111–1120
DOI 10.1007/s00535-014-0952-0

The Japanese Society of Gastroenterology

REVIEW

Interaction between gastric cancer stem cells and the tumor microenvironment

Takatsugu Ishimoto · Hiroshi Sawayama · Hidetaka Sugihara · Hideo Baba

Received: 4 February 2014 / Accepted: 5 March 2014 / Published online: 21 March 2014

Abstract Gastric cancer (GC) remains a leading cause of cancer-related deaths worldwide. Cancer stem cells (CSCs) are selectively capable of tumor initiation and are implicated in tumor relapse and metastasis, thus, governing the prognosis of GC patients. Stromal cells and extracellular matrix adjacent to cancer cells are known to form a supportive environment for cancer progression. CSC properties are also regulated by their microenvironment through cell signaling and related factors. This review presents the current findings regarding the influence of the tumor microenvironment on GC stem cells, which will support the development of novel therapeutic strategies for patients with GC.

Keywords Cancer stem cell · Tumor microenvironment · Niche · Gastric cancer

Introduction

Gastric cancer (GC) is the second-leading cause of cancer-related deaths worldwide [1]. Despite improvements in treatment, the prognosis of patients with advanced GC after curative resection remains poor, mainly as a result of tumor relapse and metastasis [2]. Increasing recent evidence has shown that tumor heterogeneity is a result of the hierarchical organization of cancer stem cells (CSCs), which are deeply implicated in tumor progression and metastasis [3–5]. Tumors have been known to show obvious histological heterogeneity since the 19th century. In 1937, Furth and Kahn revealed that a single leukemic cell was capable of transmitting systemic disease in recipient mice [6]. However, it has taken a long time for the concept of CSCs to become widely recognized. CSCs were first identified in acute myeloid leukemia (AML) by Bonnet and Dick in 1997, who found that CD34+ CD38− fractions from AML patients enhanced tumorigenicity after serial transplantation into immunodeficient mice [7]. CSCs have subsequently been identified in various types of solid tumors [8–10]. Gastric cancer stem cells (GCSCs) have recently been identified in studies of GC cell lines and primary GC tissues [11].

Solid tumors consist of cancer cells and various types of stromal cells, fibroblasts, endothelial cells, and hematopoietic cells, mainly macrophages and lymphocytes. Interactions between cancer cells and their microenvironment can have a substantial impact on tumor characteristics. Furthermore, alterations in the tumor microenvironment may also facilitate the development of tumor cell heterogeneity through the extrinsic activation of various cell signaling pathways [12, 13]. The mechanisms responsible for maintaining GCSCs in human GC have gradually been revealed (Fig. 1). This review presents the current evidence regarding the regulation of GCSCs in the tumor microenvironment.

Identification of GCSCs

Takaishi et al., identified CD44 as a potential cell surface marker of GCSCs in several GC cell lines (NCI-N87, AGS, MKN-28, MKN-45, and MKN-74). The CD44+ fraction isolated from these cell lines demonstrated a sphere-forming ability in vitro, as well as tumorigenic ability when

T. Ishimoto · H. Sawayama · H. Sugihara · H. Baba (✉)
Department of Gastroenterological Surgery, Graduate School of Medical Science, Kumamoto University, 1-1-1 Honjo, Kumamoto 860-8556, Japan
e-mail: hdobaba@kumamoto-u.ac.jp

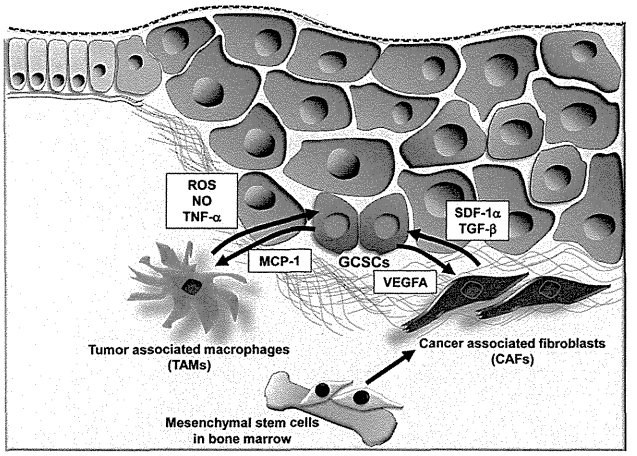

Fig. 1 Gastric cancer stem cells in the tumor microenvironment. Gastric cancer stem cells (GCSCs) exist as a subpopulation in cancer tissues, and their properties are controlled by the surrounding microenvironment. Reciprocal interactions between GCSCs and stromal cells are likely to be mediated by the indicated soluble factors. *ROS* reactive oxygen species, *NO* nitric oxide, *TNF-α* tumor necrosis factor-α, *SDF-1α* stromal-derived factor-1α, *TGF-β* transforming growth factor-β, *VEGFA* vascular endothelial growth factor A, *MCP-1* monocyte chemotactic protein-1

injected into the stomach or skin of immunodeficient mice [14]. Furthermore, Zhang et al., examined a combination of the cell surface markers CD44 and CD24 in GC cell lines and primary GC tissues from five patients using fluorescence-activated cell sorting. They found that the CD44+/CD24+ fraction exhibited higher tumorigenicity when injected into immunodeficient mice, compared with the CD44−/CD24− fraction. These cells, thus, have the capacities to both self-renew and produce differentiated progeny, which suggests that combined CD44+/CD24+ expression may act as a putative GCSC marker [15]. Chen et al., isolated CSCs from human GC tissues and the peripheral blood of GC patients using CD44 and CD54 surface markers, and generated tumors that resembled the original human tumors when injected into immunodeficient mice. The same cells differentiated into gastric epithelial cells in vitro, and self-renewed in vivo and in vitro. These results suggest that the combination of CD44+/CD54+ can also be used as a potential biomarker for GCSCs [16]. Han et al., identified the epithelial cell adhesion molecule (EpCAM) and CD44 as putative GCSC markers. The EpCAM+/CD44+ fraction from human GC tissues formed tumors in immunodeficient mice, and maintained a differentiated phenotype and reproduced the morphological and phenotypical heterogeneities of the original gastric tumor tissues. These cells had greater resistance to anti-cancer drugs than other subpopulations of cells [17]. Recently, Katsuno et al., also demonstrated aldehyde dehydrogenase 1 (ALDH1) as a candidate marker for GCSCs. ALDH1+ cells from a human diffuse-type GC cell line possessed a higher tumorigenic capacity in vitro and in vivo, compared with ALDH1− cells, and were able to self-renew and generate heterogeneous cell populations. Moreover, regenerating islet-derived family member 4 (REG4) was up-regulated in ALDH1+ GCSCs, and ALDH1 and REG4 expression were down-regulated by transforming growth factor-β (TGF-β), which correlated with a reduction in the GCSC population and tumorigenicity [18]. More recently, Liu et al., enriched GCSCs through spheroid-body formation by cultivating the human GC cell line MKN-45 in defined serum-free medium. Spheroid-body-forming cells possessed GCSC properties, including persistent self-renewal, extensive proliferation, drug resistance, high tumorigenic capacity, and overexpression of CSC-related genes and proteins (Oct4, Sox2, Nanog, and CD44), compared with the parental cells [19]. Furthermore, Jiang et al., showed that CD90+ cells possessed a greater ability to initiate tumors in vivo compared with CD90− cells, and could re-establish the cellular hierarchy of tumors from single-cell implantation, demonstrating their self-renewal properties. In addition, ERBB2 was overexpressed in about 25 % of the gastric primary tumor models, which correlated with the higher level of CD90 expression in these tumors, and trastuzumab treatment could reduce the CD90+ population in the whole tumor mass and suppress tumor growth when combined with traditional chemotherapy. Taken together, this evidence suggests that CD90 may be another potential candidate marker of GCSCs [20]. Ohkuma et al., demonstrated that the CD71− fraction in MKN1 cells was enriched after treatment with 5-fluorouracil, and accumulated during the G0/G1 cell cycle phase. This subpopulation also showed high chemoresistance to conventional chemotherapy, demonstrating its stem-cell-like properties. Limiting dilution and serial transplantation assays revealed that the CD71− cell fraction had higher tumorigenicity than the CD71+ cell fraction [21]. Jiang et al. [22] examined the expression of three putative CSC markers, ATP-binding cassette sub-family B member 1 (ABCB1), ATP-binding cassette sub-family G member 2, and CD133 in 90 human GC tissue samples and three human GC cell lines, and concluded that the expression levels of these markers in GC varied with the degree of differentiation; poorly differentiated GC expressed high levels of these markers. Furthermore, Hashimoto et al., showed that CD133 expression could be divided into two types: luminal expression in the gland, and cytoplasmic expression. Multivariate analysis revealed that expression of CD133 in the cytoplasm was an independent prognostic factor in GC [23]. The GCSC markers reported to date are summarized in Table 1. Furthermore, we previously revealed that CD44 variant isoform (CD44v), one of the cell surface markers of GCSC, contributed to defense against reactive oxygen species (ROS) by stabilizing the

Table 1 Gastric cancer stem cell markers

Cell surface markers	Phenotypes of marker-positive CSCs	Source	Correlated factors	References
CD44	Tumorigenicity, spheroid formation, chemoresistance	GC cell lines	Not reported	[14]
CD24/CD44	Tumorigenicity	GC cell lines, human GC tissues	SHH, PTCH1, GLI3	[15]
CD54/CD44	Tumorigenicity, hierarchical organization	Human GC tissues, peripheral blood	Not reported	[16]
EpCAM/CD44	Tumorigenicity, phenotypical heterogeneity, chemoresistance	Human GC tissues	Not reported	[17]
ALDH1	Tumorigenicity, phenotypical heterogeneity	Diffuse type GC cell lines	REG4, TGF-β	[18]
CD90	Tumorigenicity, trastuzumab reduce the CD90+ population	Human GC tissues	ERBB2	[20]
CD71−	Tumorigenicity, chemoresistance, tumor cell invasion	GC cell line (Adenosquamous carcinoma)	Not reported	[21]
CD133	Poorly differentiated GC, Independent prognostic factor	GC cell lines, Human GC tissues	ABCB1, ABCG2, HIF1-α	[22, 23]

glutamate-cystine transporter subunit ×CT, and promoting the synthesis of the primary intracellular antioxidant glutathione [24, 25]. These findings suggest that the other GCSC markers may not only act as cell surface markers, but may also play functional roles in tumor progression and metastasis.

Tumor microenvironment in GC

Cancer cells modify and activate their microenvironment by secreting growth factors and proteases, while stromal cells also affect cancer cells by secreting soluble factors such as growth factors or cytokines. These interactions can act in an autocrine and a paracrine manner. Among the stromal cells, myofibroblasts, also known as carcinoma-associated fibroblasts (CAFs), are large spindle-shaped mesenchymal cells that share characteristics with smooth-muscle cells and fibroblasts. CAFs have been reported to promote various types of tumor through secretion of soluble factors, including growth factors and cytokines [26, 27]. Guo et al., revealed that a subset of gastric myofibroblasts was derived from bone marrow (BM) in a transgenic mouse model of GC. Myofibroblasts stimulated by gastric tumor cells expressed vascular endothelial growth factor A (VEGFA) and other angiogenic factors, which may lead to the promotion of angiogenesis in gastric tumors [28]. Worthley et al. [29] identified BM-derived neoplasia-associated myofibroblasts in female recipients of male allogeneic stem cell transplants with GC. Quante et al. [30] showed that at least 20 % of CAFs originated from the BM and were derived from mesenchymal stem cells (MSCs), and that MSC-derived CAFs were recruited to the tumor in a TGF-β- and stromal-derived factor (SDF)-1α-dependent manner in mouse models of inflammation-induced gastric dysplasia. Furthermore, Shibata et al. [31] revealed that SDF-1α produced by myofibroblasts promoted gastric epithelial proliferation partly through CXCR4-positive gastric tissue stem/progenitor cells, and played a key role in gastric carcinogenesis.

Macrophages comprise the most abundant immune population in the tumor microenvironment and are responsible for the production of cytokines, chemokines, growth factors, proteases, and toxic intermediates such as nitric oxide and ROS. Tumor-associated macrophages (TAMs) are thought to contribute to tumor growth, tumor angiogenesis, extravasation of tumor cells, and suppression of antitumor immunity in various types of cancer [32–35]. Ohta et al., reported that macrophage infiltration into tumor tissue correlated significantly with tumor-vessel density in human GC. They found that monocyte chemoattractant protein-1 produced by human GC cells played a role in angiogenesis via macrophage recruitment and activation in human GCs and in a mouse orthotopic implantation model [36, 37]. Wu et al. [38] also provided important insights into how TAMs promote tumor-induced angiogenesis and lymphangiogenesis in GC. Oshima et al. [39] showed that K19-Wnt1 transgenic mice expressing Wnt1 in the gastric epithelial cells developed sporadic dysplastic lesions in the glandular stomach. They found nuclear accumulation of β-catenin in the macrophage-infiltrated dysplastic mucosa of the K19-Wnt1 mouse stomach, and revealed that Wnt/β-catenin signaling was promoted by macrophage-derived tumor necrosis factor (TNF)-α, which contributes to gastric tumorigenesis [40]. Yamanaka et al. [41] revealed that NF-κB activation in GC cells is enhanced by IL-1β secreted by tumor-infiltrating macrophages (paracrine) and/or carcinoma cells (autocrine), and thereby leads to increased invasive ability of GC cells through overexpression of MMP-9. Cardoso et al. [42] recently showed that

macrophages promote GC cell invasion into ECM components through enhanced proteolysis, cancer cell motility and migration. These achievements indicate that macrophages in the tumor microenvironment have important roles for GC cell invasion besides GC development. On the other hand, recent evidence has shown that lymphocytes within tumors have an effect on prognosis of GC patients. Zhuang et al., showed that IL-22-producing CD4+ T cells (IL-22+ CD4+ T cells) and Th22 cells (IL-22+ IL-17− IFN-γ− CD4+ T cells), newly discovered T cell subsets, may play important role during GC establishment and progression and may serve as a prognostic marker for poor survival [43]. They also showed that the percentages of CD8+ T cells that produce IL-17 in tumors are associated with the survival period of GC patients, and these cells promote chemotaxis of myeloid-derived suppressor cells, which might promote tumor progression [44].

GCSCs and their niche in the tumor microenvironment

Current evidence suggests that the characteristics of tissue stem cells, including pluripotency and self-renewal, are controlled by the surrounding microenvironment, referred to as the 'stem cell niche'. Tissue stem cells in the stomach are surrounded by a sheet of myofibroblasts that act as a niche and secrete different types of soluble factors, including bone morphogenetic proteins, TGF-β1, Wnt ligands, SDF-1, and matrix metalloproteinases (MMPs) [45, 46]. CSCs also rely on a similar niche, called the 'CSC niche', which regulates their proliferation and differentiation [47–50]. The CSC niche is composed of diverse cell lineages, including inflammatory cells, hematopoietic cells and BM-derived myofibroblasts, as well as vasculature, extracellular matrix, and hypoxia [51]. Hasegawa et al., recently demonstrated that CAFs significantly increased the number of spheroid colonies and the expression levels of CSC markers in scirrhous GC cell lines, OCUM-12/side population (SP) cells, and OCUM-2MD3/SP cells. This effect of CAFs was significantly decreased by TGF-β inhibitors, but not by fibroblast growth factor receptor or cMet inhibition. These data suggest that CAFs might regulate CSC properties in scirrhous GC by TGF-β signaling [52].

Hypoxia is known to play pivotal roles in cell survival, angiogenesis, tumor invasion, and metastasis, and is involved in the maintenance of self-renewal and the undifferentiated state of CSCs in various solid tumors, including glioma [53], prostate cancer [54], colon cancer [55], and ovarian cancer [56]. Liu et al. [57] reported that hypoxia-induced factor-1α (HIF-1α) contributed to hypoxia-increased drug resistance of GC cells by suppressing drug-induced apoptosis and upregulating the expression of major drug transporters. Kato et al. [58] reported that both acute and chronic hypoxia decreased the radiosensitivity of GC cells by cell cycle arrest, while reoxygenation enhanced the radiosensitivity of hypoxic cells. Moreover, recent studies showed that hypoxia stimulated the epithelial-mesenchymal transition (EMT) in GC cells via autocrine TGF-β/TGF-β receptor signaling, while intratumoral hypoxia promoted immune tolerance by inducing regulatory T cells via TGF-β1 [59, 60]. Matsumoto et al. [61], however, demonstrated that HIF-1α downregulated CD133 expression and that mTOR signaling was involved in the expression of CD133 in GC cells. Taken together, these studies suggest that hypoxia and the related signaling may contribute to the characteristics of GCSCs, though the underlying mechanisms remain unknown.

Recent evidence demonstrated that CSCs live within a microscopic protective niche formed by blood vessels, called the 'vascular niche', which promotes their stem-like and tumorigenic states. Vascular endothelial cells have been identified as a critical component of the CSC niche. Calabrese et al., showed that brain CSCs were located nearer to the tumor vasculature than non-stem-like tumor cells in brain tumor xenografts [57]. They further showed that human primary endothelial cells interacted selectively with brain CSCs in culture, and secreted factors to support the maintenance and expansion of stem-like tumor cells in vitro, and to promote their tumorigenicity. In contrast, depletion of blood vessels from xenografts ablated self-renewing cells from tumors and arrested tumor growth [62]. These data indicate that the tumor vasculature may be essential for supporting and preserving the stem-like properties and expansion of CSCs, which are in turn critical for their ability to cause tumor progression. Ritchie et al. [63] also demonstrated that CSCs in head and neck squamous cell carcinoma localize preferentially at the invasive fronts in close to tumor vasculature, in an area functionally defined as the perivascular niche. As for GC, the Avastin in Gastric Cancer (AVAGAST) trial was designed to evaluate the efficacy of adding bevacizumab, a humanized anti-human VEGFA monoclonal antibody, to capecitabine-cisplatin as first-line treatment for advanced GC. This trial demonstrated that the addition of bevacizumab to chemotherapy was associated with significant increases in progression-free survival and overall response rate, but not with overall survival [64]. Singh et al. [65] recently showed that trastuzumab in combination with VEGF-Trap binding to VEGFA, VEGFB, and placental growth factor, may represent an effective approach to treating HER2-overexpressing GCs.

Vasculogenic mimicry (VM) has been identified as a new pattern of tumor neovascularization characterized by the acquisition of endothelial cell markers and the formation of vascular channels by tumor cells. VM has been observed in dysregulated melanoma and several other types

of malignancies [66–70] and is associated with an undifferentiated tumor cell phenotype and poor prognosis, suggesting that CSCs may be more likely than other tumor cells to participate in this process [71–73]. Li et al. [74] revealed that VM occurs in GC, especially in poorly differentiated GC, and was related to unfavorable prognosis. Jiang et al. [75] showed that IRX1 overexpression effectively suppressed peritoneal spreading and pulmonary metastasis via anti-angiogenesis and anti-VM mechanisms, in addition to its previously known effects on cell growth and invasion. These data indicate that the tumor vasculature may play an important role in the GCSC niche, and suggest that further research into the molecular mechanisms of VM may lead to new therapeutic strategies aimed at GCSCs.

Regulation of GCSCs via cell signaling pathways

The proliferation and differentiation of tissue stem cells are regulated by intracellular signaling pathways. Dysregulation of these pathways allows the transformation of normal cells and the gradual development of cancer [76]. Recent evidence has revealed that overexpression of stem cell regulators is closely implicated in GC development [77–79]. CSCs and tissue stem cells possess several similarities in terms of their dependence on responsible signaling pathways, and the effects of extrinsic factors from the microenvironment on intracellular signaling [80–83].

Wnt signaling can be divided into canonical and non-canonical pathways. In canonical Wnt signaling, Wnt ligands bind Frizzled receptors, β-catenin phosphorylation is suppressed leading to its stabilization and nuclear translocation, and target-gene transcription is, thus, activated by the interaction of β-catenin with transcriptional factors. The non-canonical Wnt pathway is independent of β-catenin accumulation and regulates crucial events during embryonic development.

Both of these Wnt signaling pathways have been found to play important roles in the process of carcinogenesis in several types of cancer [84], including GC [85–89]. Wnt signaling in colon cancer is characterized by a gradient, in which colon CSCs are functionally marked by high levels of Wnt activity, whereas differentiated cells show markedly lower levels of Wnt activity [90]. Cai et al. [91] demonstrated that blocking Wnt signaling with the Dickkopf homolog 1 protein reduced the self-renewing capacity of MKN45 tumor-sphere cells. Furthermore, Oshima et al., showed that K19-Wnt1 transgenic mice expressing Wnt1 in the gastric mucosa under the control of the keratin 19 promoter showed significant suppression of epithelial differentiation with small preneoplastic lesions. They then crossed K19-Wnt1 mice with another transgenic line (K19-C2mE) that expresses both COX-2 and mPGES-1 in the gastric mucosa and generated transgenic line K19-Wnt1/C2mE. Notably, simultaneous activation of both the Wnt and prostaglandin E2 (PGE2) pathways caused the development of large dysplastic gastric tumors through the metaplasia-carcinoma sequence. [39]. We found that a gastric gland located at the squamo-columnar junction in normal mouse stomach contained CD44+ stem cell-like slow-cycling cells, which expanded concomitantly with tumor development in K19-Wnt1/C2mE mice. These findings suggest that Wnt signaling cooperatively promotes PGE2-induced CD44+ gland cell expansion in gastric tumorigenesis [92]. Furthermore, Oguma et al. [40] detected β-catenin nuclear accumulation in macrophage-infiltrated dysplastic mucosa in the K19-Wnt1 mouse stomach, and showed that macrophage-derived TNF-α promoted Wnt signaling through inhibition of glycogen synthase kinase-3β, which may contribute to tumor development in the gastric mucosa. These results suggest that GCSC regulation through Wnt signaling is mediated by the surrounding immune cells.

Notch signaling is a crucial determinant of cell fate during development, stem cell self-renewal, and postnatal tissue differentiation [93–95]. Increasing evidence suggests that deregulation of Notch signaling occurs frequently and is implicated in the CSC properties in several types of human malignancies [96–98]. Yeh et al. [99] demonstrated that activation of the Notch1 signaling pathway promoted GC progression partially through COX-2. Piazzi et al. [100] revealed that Notch1 activity in GC was regulated by epigenetic silencing of the Notch1 ligand DLL1, and that Notch1 inhibition was associated with diffuse-type GC. However, the functional roles and regulatory mechanisms of Notch signaling in GCSCs remain largely unknown, and further studies are needed.

The Hedgehog family of secreted proteins orchestrates a wide variety of processes during embryonic development and adult tissue homeostasis. There are three known vertebrate Hedgehog family ligands: Sonic hedgehog (SHH), Indian hedgehog (IHH), and Desert hedgehog (DHH). Among these, SHH is expressed in the fundic glands in the human stomach, and SHH upregulation leads to carcinogenesis through aberrant activation of the Hedgehog signaling pathway in GCs [101, 102]. Furthermore, Yoo et al. [103, 104] demonstrated that SHH promoted motility and invasiveness of GC cells through TGF-β-mediated activation of the activin receptor-like kinase 5-Smad 3 pathway. SHH signaling also promoted GC metastasis through activation of the PI3K/Akt pathway, which leads to mesenchymal transition and MMP-9 activation. Zhang et al. [15] found that the CD44+/CD24+ fraction exhibited higher tumorigenicity when injected into immunodeficient mice, and SHH, PTCH1, and GLI3 mRNA expression levels were significantly increased in this subpopulation.

Song et al. determined that GC cell lines (HGC-27, MGC-803, MKN-45) grown in a defined serum-free medium could form tumor spheres containing cells that behaved like GCSCs, and that the expression levels of SHH-pathway target genes (Ptch and Gli1) were significantly higher in tumor-sphere cells than in adherent cells. Tumor spheres from GC specimens also showed chemoresistance and tumorigenic capacity, and the SHH pathway maintained the GCSC characteristics of tumor-sphere cells from primary tumor samples [105]. These findings suggest that the SHH pathway may be involved in the self-renewal, proliferation, drug resistance and tumorigenicity of tumor-sphere cells, and inhibition of the SHH pathways may, thus, represent a rational therapeutic target aimed at GCSCs. However, the mechanisms underlying the regulation of SHH signaling have not been clarified, and further analysis is required to determine the underlying mechanisms.

Regulation of GCSCs through microRNAs

MicroRNAs (miRNAs) are non-coding RNAs of 21–25 nucleotides in length that repress mRNA translation by base-pairing to partially complimentary sequences in the 3′-untranslated region (UTR) of their target mRNAs. Accumulating evidence suggests that dysregulation of miRNAs is deeply involved in the pathogenesis of many cancers, and that a network of miRNAs regulate CSC properties [106, 107]. Recent studies have revealed that various miRNAs regulate putative GCSC-marker expression and are associated with an unfavorable prognosis (Table 2). Ueda et al. [108] demonstrated that low expression of let-7g and miR-433 and high expression of miR-214 were associated with unfavorable outcomes in terms of overall survival, based on miRNA microarray analysis of 101 samples from GC patients who underwent curative surgery, and their associated prognostic information. Zheng et al. [109] showed that miR-148a suppressed tumor cell invasion and lymph node metastasis by down-regulating ROCK1 in GC cell lines and in 90 GC samples. Gao et al. [110] demonstrated that miR-145 suppressed GC cell metastasis by inhibiting the protein translation of its direct target gene N-cadherin, and may then indirectly down-regulate its downstream effector MMP9. In contrast, the miR-200 family has been reported to induce epithelial differentiation and suppress EMT by inhibiting translation of zinc finger E-box-binding homeobox (ZEB) 1 and 2 mRNAs in several types of cancers. Kurashige et al. [111] showed that miR-200b suppressed ZEB2 expression and may, thus, regulate metastasis in GC. Song et al. identified miRNA-based GC subtypes by consensus cluster analysis of miRNA profiles of 90 GC tissues. The poor-prognosis GC miRNA subtype was characterized by overexpression of EMT markers, and three miRNAs (miR-200c, miR-200b, and miR-125b) driving the GC mesenchymal subtype in the network were significantly associated with survival [112]. Tumor cells undergoing EMT are known to acquire CSC-like properties, including enhancement of

Table 2 Dysregulation of microRNAs in gastric cancer

miRNA expression	Target genes	Source	Phenotyes	Correlated factors	References
let-7g↓, miR-433↓, miR-214↑	HMGA2, GRB2, PTEN	Human GC tissues	Poor prognosis	Not reported	[108]
miR-148a↓	ROCK1	GC cell lines, human GC tissues	Tumor cell migration and invasion, lymph node-metastasis	Not reported	[109]
miR-145↓	N-cadherin	GC cell lines, human GC tissues	Tumor cell migration and invasion, metastasis	MMP9	[110]
miR-200b↓	ZEB2	GC cell lines, human GC tissues	Tumor cell migration and invasion, metastasis	E-cadherin	[111]
miR-200c↓, miR-200b↓ miR-125b↓	ZEB1	GC cell lines, human GC tissues	Mesenchymal subtype, poor prognosis	E-cadherin	[112]
miR-15b↓, miR-16↓	BCL2	GC cell lines	Multidrug resistance	Not reported	[114]
miR-106a↑	RUNX3	GC cell lines	Multidrug resistance	Not reported	[115]
miR-508-5p↓	ABCB1, ZNRD1	GC cell lines, human GC tissues	Multidrug resistance	Not reported	[116]
miR-7↓	Not reported	K19-C2mE, gan mouse models	Cell proliferation, soft agar colony formation	IL1-β, TNF-α	[117]
miR-328↓	CD44	GC cell lines, human GC tissues	Tumorigenicity, chemoresistance	Macrophage, ROS	[118]
miR-30e*↓	Bmi1	GC cell lines, human GC tissues	Sphere formation	Macrophage	[119]